Energy Saving Potential of a Self Learning Thermal Comfort System in Dutch Residential Dwellings

de Louw, K.G.W.M.

Award date:
2018

University of Technology Eindhoven
AME

Energy Saving Potential of a Self Learning Thermal Comfort System in Dutch Residential Dwellings

Graduation Thesis
Sustainable Energy Technology

Author: K.G.W.M. de Louw, BSc. - 0814690
Supervisors: prof. dr. ir. D.M.J. Smeulders
T.J.H. Langerwerf, BSc.

Department: Mechanical Engineering
Research Group: Energy Technology

November 16, 2018

Technische Universiteit
Eindhoven
University of Technology

Declaration concerning the TU/e Code of Scientific Conduct for the Master's thesis

I have read the TU/e Code of Scientific Conduct[i].

I hereby declare that my Master's thesis has been carried out in accordance with the rules of the TU/e Code of Scientific Conduct

Date

16-11-2018

Name

K.G.W.M. de Louw

ID-number

0814690

Signature

K.deLouw

Submit the signed declaration to the student administration of your department.

[i] See: http://www.tue.nl/en/university/about-the-university/integrity/scientific-integrity/
The Netherlands Code of Conduct for Academic Practice of the VSNU can be found here also.
More information about scientific integrity is published on the websites of TU/e and VSNU

Acknowledgements

This thesis concludes my graduation project of the master Sustainable Energy Technology, and therefore my time at Eindhoven University of Technology. First of all, I would like to express my great appreciation to prof.dr.ir. D.M.J. Smeulders, for taking part in this project as my supervisor. Furthermore, I am particularly grateful for the valuable feedback of my company supervisor T.J.H. Langerwerf, BSc. I would also like to thank AME for giving me the opportunity to carry out a really interesting research, which may be a valuable step in accelerating the energy transition. Finally, I want to show my gratitude to all the people who supported me during my student career.

Abstract

This study investigated an uncommon approach of controlling the thermal environment in Dutch residential buildings. A centralised data-driven HVAC controller was developed, in order to optimise energy usage while maintaining a thermally comfortable environment. This Economic Model Predictive Controller (EMPC) is integrated in a building based on Dutch reference dwellings with EPC-0.4. It only uses simulated data in order to identify a temperature forecast model. The identified model was used to perform a forecast over the next 24 hours, which is used to perform optimisation cycles over control actions in a receding horizon fashion.

Several scenarios are developed with a combination of Dymola and Simulink, in which the controller is analysed. The coupling between Simulink and Dymola has been established with the Functional Mockup Interface (FMI). This made detailed house models possible, while using the advanced control possibilities of Matlab/Simulink. Generally, the controller shows acceptable thermal and economic performance, and is therefore a promising method for future residential climate control. Still, the performance of the forecast model has still much room for improvement.

List of Abbreviations

Abbreviation	Description
MPC	Model Predictive Control
EMPC	Economic Model Predictive Control
EPC	Energy Performance Coefficient
COP	Coefficient of Performance
PMV	Predicted Mean Vote
RH	Relative Humidity
ATCS	Adaptive Thermal Comfort System
ARX	AutoRegressive model with eXogenous inputs
BPS	Building Performance Simulation
FMU/FMI	Functional Mockup Unit / Functional Mockup Interface
HVAC	Heating, Ventilation and Air-conditioning
RVO	Rijksdienst Voor Ondernemend Nederland
HP	Heat pump

Contents

Chapter 1: Introduction

The latest climate report by the Intergovernmental Panel on Climate Change (IPCC) warns for devastating consequences if global warming exceeds 1.5°C compared to pre-industrial temperatures. In order to prevent exceeding this temperature level, CO_2 emissions should drop with 45% from 2010 levels by 2030, and be net zero by 2050 [1]. The European Union adopted the new Directive 2018/844, which states that greenhouse gas emissions should be reduced at least by 40% in 2030, compared with 1990's levels. What is more, building stock is responsible for 36% of all CO_2 emissions, and should be fully de-carbonised by 2050 [2]. The *New Stepped Strategy* by Van den Dobbelsteen (2009) [3] formulates four steps to reduce the greenhouse gas emissions, namely:

1. Reduce consumption.
2. Reuse waste energy streams.
3. Use renewable energy sources and ensure that waste does not disturb the environment, or is reused as food.
4. Supply the remaining demand cleanly and efficiently.

This research will focus on the first step, by utilising smart control solutions within residential buildings. Almost 40% of the total energy consumption is accounted for heating and cooling buildings [2]. In 2015 the total heating energy required for households in the Netherlands was 327 PJ, of which 289 PJ was generated by combustion of natural gas; for cooling in 2015 the required energy was 1 PJ (CBS, 2017) [4]. In the present thesis, a control type which is already well established in chemical plants and oil refineries [5], is utilised to control heating and cooling systems in Dutch residential buildings. This Model Predictive Controller (MPC) uses a self-learning model to centrally control the heating system, ventilation system, and solar shading system, while maintaining a thermally comfortable environment, in an economically efficient way.

First, a literature study is performed to research the criteria, the current state of research, and the required capabilities of the control system. Second, an analysis is carried out to select a proper simulation environment to develop the controller, and to develop a Dutch reference building. Finally, the methodology is established and the controller performance is assessed.

Chapter 2: Literature Study

This chapter presents the current state of research in thermal comfort, thermal comfort prediction, and model predictive control strategies. First, background information about thermal comfort (prediction) is given; second, important key elements in climate control are discussed, and finally several adaptive model predictive control strategies are explained.

2.1 Thermal Comfort

Thermal comfort is a subjective factor which varies from person to person. Therefore, correctly modelling this parameter is quite difficult. The most popular model is the Predicted Mean Vote (PMV) model [10], which was developed in the late 1960s. It is adapted in the ASHRAE Standard 55 - Thermal Environmental Conditions for Human Occupancy. It correlates environmental parameters such as: air temperature, air velocity, relative humidity, and radiant temperature. Furthermore, personal parameters are included such as: metabolism and clothing. The levels of comfort are based on a scale between -3 and 3, which means very cold, and very hot, respectively. The human body is thermally satisfied when the PMV value is between -0.5 and 0.5. However, the personal parameters are (until now) difficult to measure, and therefore these parameters are often assumed to be constant default values [7]. In addition, if the occupant cannot (properly) control the thermal environment, the discomfort increases [6] [12].

Mohammad et al. (2016) [7] shows that the effect of the personal parameters far exceeds that of the environmental factors, within normal parameter ranges (RH 30%-60%, indoor temperature: 15-32 °C). However, with recent developments in wearable devices such as smart watches, and health monitoring devices the level of metabolism can be measured easily. This leads to opportunities for smart energy systems to estimate the thermal comfort temperature range more accurately. On the other hand the relative humidity is rarely in need of monitoring, because the PMV model is not sensitive on the normal parameter ranges, compared to the metabolism [7].

Alders et al. (2011) [11] stated that it is essential to determine a temperature range (±2 °C) under which occupants feel comfortable, rather than focussing only on a single temperature value [12]. In addition, the thermal sensitivity of people may vary from person to person. Therefore, there is no fixed optimal temperature which satisfies all occupants in a dwelling. By combining detailed weather data, and detailed occupancy profiles one can create detailed comfort demand profiles [11].

Van Hoof et al. (2010) [20] found that for naturally ventilated buildings the indoor temperature is lower in colder climate zones, including the Netherlands, than for air-conditioned buildings. Apart from that, occupants of fully air-conditioned buildings are twice as sensitive to fluctuations in temperature as occupants of naturally ventilated buildings [20]. This may result in a (additional) higher energy demand for air-conditioned buildings.

In order to reduce the heating demand in a building, insulation can be installed. However, this can lead to overheating problems during summer. As a result, residents may install cooling devices, which leads to an increase in energy demand of the building. The overheating problems mainly occur due to trapped heat produced by solar radiation, and internal heat gain. Therefore, both heating and cooling seasons should be assessed. To reduce the total energy demand, and optimise the thermal comfort in a dwelling, an Adaptive Thermal Comfort System should be developed [6].

2.2 Adaptive Thermal Comfort System

According to Alders (2016) [6] an Adaptive Thermal Comfort System (ATCS) can be defined as: *"The whole of passive and active comfort components of the dwelling that dynamically adapts its*

settings to varying user comfort demands and weather conditions (seasonal, diurnal and hourly depending on the aspects adapted), thus providing comfort only where, when and at the level needed by the user, to improve possibilities of harvesting the environmental energy (e.g. solar gain and outdoor air) when available and storing it when abundant". Energy saving during the heating season is relatively simple with this kind of system. The saving potential is around 50% when high thermal insulation is applied, the construction is very airtight, and the ventilation losses are minimized by the system. When solar gain is optimised during winter the saving potential increases to 80%. During summer season the system should use solar shading in order to reduce thermal gain within the building. In addition, controlled solar shading combined with controlled (natural) ventilation can effectively eliminate the need for active cooling in Dutch dwellings. Which leads to a saving potential of almost 100% for cooling energy demand. Furthermore, vents can be made smaller which reduces costs, and decreases the risk of draught [6].

2.2.1 Thermal Comfort Prediction

There are three possibilities to model thermal comfort; 1. The PMV model [10], 2. Adaptive thermal comfort models [23], 3. Personal comfort model [21]. According to Kim et al. (2018) [21] the latter performed generally 43% better than the other two options. On average the machine learning algorithms used in the study converged after 64 survey responses of the occupants. This is a limiting factor for models that depend on survey feedback to train itself.

The PMV model is initially designed for office buildings, however the range of variables in residential buildings is wider than for office buildings. In addition, Alders (2016) [6] stated that occupants should be able to create their own environment in their home, which should be facilitated by the comfort system. Therefore, Peeters et al. (2009) [23] already proposed to divide the residence in three different zones; the bathroom, bedrooms, and other rooms. In the same research it was stated that thermal comfort in residential buildings strongly depends on recent outdoor temperatures. The proposed adaptive comfort model [23] is defined in Equations 2.1 2.2 2.3 2.4 2.5 2.6. The model is based on previous work of Van der Linden et al. (2006) [22], which is used for Dutch official residential building purposes [13].

Weighted average outdoor temperature:

$$T_{e;ref} = \frac{T_{t=today} + 0.8 \cdot T_{t=today-1} + 0.4 \cdot T_{t=today-2} + 0.2 \cdot T_{t=today-3}}{2.4} \tag{2.1}$$

where T_t is the average between the minimum and maximum temperature of that specific day.
Bedroom:

$$T_n = \begin{cases} 16^{\circ}C & \text{for } T_{e;ref} < 0^{\circ}C \\ 0.23 \cdot T_{e;ref} + 16 & \text{for } 0^{\circ}C \leq T_{e;ref} < 12.5^{\circ}C \\ 0.77 \cdot T_{e;ref} + 9.18 & \text{for } 12.6^{\circ}C \leq T_{e;ref} < 21.8^{\circ}C \\ 26^{\circ}C & \text{for } T_{e;ref} \geq 21.8^{\circ}C \end{cases} \tag{2.2}$$

$$\begin{aligned} T_{comfort,\,max} &= min(26^{\circ}C,\ T_n + \omega \cdot \alpha) \\ T_{comfort,\,min} &= max\big(16^{\circ}C,\ T_n - (1-\alpha) \cdot \omega\big) \end{aligned} \tag{2.3}$$

Bathroom and other rooms:
T_n bathroom:

$$T_n = \begin{cases} 0.112 \cdot T_{e;ref} + 22.65 & \text{for } T_{e;ref} < 11^{\circ}C \\ 0.306 \cdot T_{e;ref} + 20.32 & \text{for } T_{e;ref} \geq 11^{\circ}C \end{cases} \tag{2.4}$$

T_n other rooms:

$$T_n = \begin{cases} 0.06 \cdot T_{e;ref} + 20.4 & \text{for } T_{e;ref} < 12.5^{\circ}C \\ 0.36 \cdot T_{e;ref} + 16.63 & \text{for } T_{e;ref} \geq 12.5^{\circ}C \end{cases} \tag{2.5}$$

$$
\begin{aligned}
T_{comfort,\,max} &= T_n + \omega \cdot \alpha \\
T_{comfort,\,min} &= max\big(18°C,\; T_n - \omega \cdot (1-\alpha)\big)
\end{aligned}
\tag{2.6}
$$

where $\alpha = 0.7$ is a statistical constant, and $\omega = 5°C$ is the width of the comfort band, with a Predicted Percentage of Dissatisfied (PPD) value of 10%. T_n is the statistical neutral temperature, $T_{e;ref}$ the outdoor reference temperature, and $T_{comfort,\,max}/T_{comfort,\,min}$ the comfort limits.

The room temperature in this study is defined as the operative temperature, which is based on the mean radiant temperature, and the mean zone air temperature. The operative temperature is computed with Equation 2.7.

$$
T_{op} = \gamma T_{mrt} + (1-\gamma) T_{air} \tag{2.7}
$$

where γ is the radiative fraction, which has a typical value of 0.5 in residential buildings [13], T_{mrt} is the mean radiant temperature, and T_{air} is the mean zone air temperature.

The adaptive comfort model does not actively implement thermal comfort factors described by Fanger, such as metabolic activity, clothing level, air velocity, and humidity (PMV model) [10] [13]. Moreover, the field test of Ioannou et al. (2017) [14] found that neutral temperatures for dwellings with an F-rating were lower than the dwellings with an A/B-rating, which was explained by the higher air velocities of the ventilation systems. Consequently, energy performance is not as high as one would expect, based on the energy ratings.

2.2.2 Controlled Ventilation

Ventilation is required to maintain a healthy indoor climate, by removing moisture, CO_2, and other pollutants. Poor indoor air quality can cause a large range of medical issues. Especially in the last decades, when buildings became more and more airtight, this led to the Sick Building Syndrome [8]. In addition, ventilation can be used to lose indoor heat to the outdoor environment. A dwelling can be ventilated with natural or mechanical ventilation systems. Vent openings above windows and doors enable the use of natural ventilation, without using additional energy for fans. Consequently, energy is only used to remotely control the openings. During winter, heat loss can be reduced by using a heat recovery unit in the mechanical ventilation system. Meanwhile ventilation levels should be minimised as much as possible in all cases, while maintaining healthy conditions [6].

2.2.3 Controlled Solar Shading

Thermal energy is transferred through windows by solar radiation. The amount of solar radiation can be controlled by using shading devices (e.g. hatches). However, this may block or alter the view of the occupants, which may be a major drawback [6]. The ATCS should be able to measure the amount of solar radiation, and act accordingly.

2.2.4 Automation to Prevent Overheating

Alders (2016) [6] researched automation strategies of ventilation, and solar shading, and concluded that automation of adaptive solar gain gives the highest reduction in overheating. The overheating reduction of fully controlled ventilation is significant, but considerably less than automated adaptive solar gain. The research assumed that the ventilation, and solar gain system is correctly controlled during occupied hours by the occupants. Furthermore, the effect of automation is larger in a building with low thermal mass, because of the damping effect of thermal mass on the temperature.

2.2.5 Adaptive Model Predictive Control

Model predictive control (MPC) has shown that it is capable of achieving higher energy efficiency in buildings than conventional control strategies. However, it is not possible to use this in commercial products, because these control techniques heavily rely on a perfect model of the building, and a perfect estimation of the system's dynamics. Every building needs an adapted model in order to get usable predictions. Therefore an adaptive MPC can be developed, which is adapting its parameters autonomously in order to correctly predict the thermal behaviour [9] [15]. This results in robustness, tunability, and flexibility of the model. Field tests of an adaptive model predictive controller yielded energy savings of 28 $\pm$4%, compared to weather-compensated heating controllers [9]. Furthermore, the energy saving potential is up to 41% when compared to conventional rule-based controllers [15]. However, during the adaptation phase, severe comfort constraint violations may occur until the parameters converge [17].

Maasoumy et al. (2014) [15] proposed a parameter adaptive building (PAB) model, and designed a robust MPC for buildings. This PAB model is capable of tuning its parameters in an online and automatic fashion. Each timestep it uses an unscented Kalman filter to estimate the state and the parameters of the system, in order to calculate the temperature at n+1. The PAB strategy is a promising method to remove model uncertainty. Tanaskovic et al. (2017) [17] proposed a robust, adaptive MPC, which achieved to satisfy comfort criteria even during the adaptation phase.

Another control strategy is Batch Reinforcement Learning (BRL), which is a model-free (e.g. no model for building dynamics available) data-driven approach based on machine learning techniques. With this strategy the policy is calculated with historical data. Costanzo et al. (2016) [16] showed that such a strategy can achieve a performance within 90% of the mathematical optimum (MPC with a correct building model). Ferracuti et al. (2017) [18] reviewed other data-driven strategies, and concluded that an AutoRegressive model with eXogenous inputs (ARX) is capable of predicting the room temperature with an error of 0.8°C, with a time horizon of 3 hours. The advantage of model-free strategies is that model inaccuracies are not inherited by the target, because data of the target itself is used. These inaccuracies in model-based approaches become larger as time evolves [19].

The last method discussed here is a generalized online transfer learning algorithm (GOTL), proposed by Grubinger et al. (2017) [24]. In general, transfer learning methods aim at transferring knowledge from source models to a target model, with limited training data of the target. In climate control systems of residential buildings, the knowledge transfer should be implemented in an online manner, so the model can train itself after installation. An Online Transfer Learning method uses a weighted prediction of an offline classifier, which is trained from source data over an extended time horizon. The proposed algorithm consists of an offline linear regression model, and an online regressor. The online regressor is trained and updated on the target house during operation. This type of algorithm is capable of predicting the thermal dynamics in residential buildings, with source data collected from other (nonsimilar) houses [24].

Chapter 3: Simulation Tools

In order to assess a Dutch residential building, and its energy system, a building performance model should be simulated. There are various simulation tools available for Building Performance Simulation (BPS). Some tools are discussed in this chapter, so a decision can be made, which tool(s) will be used in this project.

3.1 Modelica

Modelica is an equation-based, object-oriented modelling language. The main difference with often used imperative programming languages (e.g. MATLAB, C++) is that equation-based languages declare relations among variables. The computer generates the simulation code by using computer algebra. This leads to efficient code for simulation and optimisation, and the user does not need to have additional knowledge about optimal programming [25]. What is more, the user does not have to define the sequence of the code/equations. The advantage is that existing models are more easy to extend, compared to models written in imperative languages. The equations are implemented into acausal block diagrams, which represents an element of one or more physical domains (e.g. thermal or mechanical) [34]. Moreover, equation-based languages support automatic conversion of simulation models into optimisation problems, which saves costs and time. Wetter et al. (2016) [25] showed that the optimisation performance can be up to 2200 times higher than conventional gradient-free optimisation methods.

In addition, an international project comprised of 41 institutes from 16 countries called Annex 60 provides free open-source, models and components based on Modelica, Functional Mock-up Interface, and Building Information Modelling standards. The Buildings Library of Lawrence Berkeley National Laboratory [37] is part of this project. Hence, this library can be combined with other libraries of Annex 60. Annex 60 [26] reported several reasons to use Modelica, and several drawbacks, the reasons applicable to this graduation project are stated here:

Advantages:

- Flexible and extensible object-oriented modelling approach.
  This provides a high working efficiency and gives a clear view on the component and system models. It results in highly reusable components which can be easily implemented. The hierarchical structure supports system models with different levels of detail in sub-models. Existing (component) models can be combined in new system models, which are normally not available in existing simulation tools. Moreover, the model can gain a higher level of detail by just replacing a sub model, which is done by Zuo et al. (2016) [36].
- Acausal equation-based modelling approach.
  This approach leads to an easy understanding, and a good insight into the physics of the model. The equations can be written as differential-algebraic equations (DAE), while causal modelling approaches (like Simulink) use ordinary differential equations (ODE).
- Numerical reasons.
  There is a clear separation between the physical-technical model and its numerical solution, due to the automatic translation of the Modelica model into a simulation model.
- External interfaces to Modelica.
  Due to the implemented Functional Mock-up Interface (FMI) standard, Modelica models can be coupled with other simulation tools.

Drawbacks:

- Long simulation times for detailed whole building simulation.
  These kind of simulations are often slower than dedicated building energy simulation (BES) tools. Which can be explained by the following reasons (for a more elaborate list of reasons, see [26]):

  - Modelica models often include more detail, compared to EnergyPlus or TRNSYS simulation models.
  - The same time step is used for all equations. However, the time step for heat conduction in buildings can be much larger than for control loops. A promising solution is a multi-rate solver with error control.

  Nonetheless, these reasons are not an inherent problem of Modelica, and development is ongoing to solve these issues. The model itself does not (or only minor) require changes if (some of) these problems are solved, due to earlier discussed separation.
- Fewer validated models than established building simulation programs. Although, with the Annex 60 library, a large validated open-source model is available. Moreover, Modelica libraries are more transparent than e.g. EnergyPlus libraries.

Furthermore, Wetter et al. (2006) [25] carried out a comparison between Modelica and TRNSYS, and showed that the model development time is five to ten times faster with Modelica than with TRNSYS. Nevertheless, the simulation time is three to four times shorter with TRNSYS.

3.2 EnergyPlus

EnergyPlus is a free, open-source whole building energy simulation tool, developed by the U.S. Department of Energy [27]. It is seen as one of the most advanced, publicly-available building energy simulation tools. A free open-source graphical user interface is available (OpenStudio) [28]. Communication with the simulation engine occurs via text files. It has the following (non-exhaustive) features [29]:

- Integrated, simultaneous solution.
  The thermal response of the building is tightly coupled to the primary and secondary systems.
- User-definable time steps.
- ASCII in-, and output files.
- Heat balance based solution.
- Transient heat conduction through building elements.
- Combined heat and mass transfer.
- Thermal comfort models.
- Advanced fenestration calculation e.g. for window blinds.
- HVAC systems.
- Atmospheric pollution calculations.

Controllers can be represented in EnergyPlus as models of supervisory control [30].

3.3 Matlab - Simulink

Matlab is a programming platform, which is designed for engineers and scientists. It has a large set of toolboxes, like optimisation-, and machine learning toolboxes. Simulink can be used among others to model, and simulate physical systems, and design controllers. Furthermore, it can be used to deploy code for direct use on embedded systems [31]. The current controllers for smart thermostats developed at AME are created with Simulink.

3.4 Co-simulation with FMI

"Functional Mock-up Interface (FMI) is a tool independent standard to support both model exchange and co-simulation of dynamic models using a combination of xml-files and compiled C-code" [32]. This enables users to use different tools, each tailored to their own specialisation. The tools discussed here all support this standard, which means that in theory all tools can be used,

and coupled to each other. The co-simulation coupling works via a master-slave configuration, where the different simulation tools act as a slave. If a tool supports the FMI standard it contains functionality to import and/or export Functional Mock-up Units (FMU). These units contain all information to simulate the model with another application. If the tool only supports the FMU export feature, it is called a slave simulator, if it only supports FMU import, it is called a master simulator. If a tool supports both features, it is possible to create a FMU with nested FMUs. The master simulator handles all communication between the slave components [33].

Co-simulation enables the user to open a separate simulation instance for every model, therefore two models can be simulated in parallel with different solver algorithms and step sizes, this is called multi-rate simulation [34]. Musić et al. [35] did a comparison between Simulink and Modelica, and concluded that Modelica was in favor of designing models due to the reusability of other models. On the other hand, Simulink offers a wide range of toolboxes designed for control. Therefore, combining these tools would result in a powerful tool for modelling and simulation of both simple and complex systems.

Chapter 4: Project Definition

4.1 Objective

The objective of this study is to obtain the energy saving potential of a self-learning MPC with centralised control of HVAC systems. The study will focus on developing a Dutch residential building model, which is occupied according to an occupancy profile of Alders (2016) [6], based on Dutch statistics (NIWI, 2002). The used profile is given in Appendix A. The performance is assessed by varying properties like: positioning of windows, type of heating system, and uncertainty of future disturbances. The building will be exposed to Dutch weather conditions. The internal controller model predicts the behaviour of the artificial dwelling, and executes an optimisation cycle, in order to minimise the energy usage, while maintaining thermal comfort. The internal controller model should be able to predict the future temperature profile by combining primary heating (central heating system), secondary heating (e.g. solar gain, and internal gains), and ventilation. The adaptive thermal comfort model proposed by Peeters et al. (2009) [23], which is stated in Chapter 2.2.1, will be used to determine the level of thermal comfort.

4.2 Approach

From the analysis of several simulation tools in Chapter 3, a combination of Modelica and Simulink is promising in achieving the objective of this study. The building will be modelled in Modelica/Dymola, by using the validated and well documented Modelica Buildings library [37] of Lawrence Berkeley National Laboratory, which is free to use. The dwelling is based on reference buildings prescribed by *Rijksdienst voor Ondernemend Nederland (RVO)* [38]. The controller, and machine learning algorithm will be developed with Matlab/Simulink. Simulation data of the building model is used to train the algorithm. Afterwards the accuracy of the trained model will be assessed by comparing the simulation data of the virtual building with the data of the trained algorithm. This data-driven model will then be implemented in an MPC controller, which controls the following aspects:

- Heating by a generic heat pump
- Ventilation
- Solar shading

The optimisation problem should minimise the energy usage by the heat pump, while maintaining thermal comfort.

Chapter 5: Methodology

This chapter describes the methodology used in this thesis, hence one should be able to replicate the research by following this chapter. Firstly, it presents the data-driven structure used by the MPC; secondly, the artificial building, and its model structure is given; thirdly, the developed optimisation algorithm is described, and finally, all components are coupled within a Simulink model.

5.1 Data-driven Model (ARX)

A Model Predictive Controller requires a model of the controlled plant. An AutoRegressive model with eXogenous inputs (ARX) model is identified in order to forecast the future response of the building. In Equation 5.1 the general structure of an ARX model is given. This is a linear model, which helps to reduce computational costs during control optimisation. In this thesis the distinction is made between the ARX-based model, and the modelica model. The ARX-based model acts as the internal model for the MPC; which is able to make forecasts over the near future. The modelica model acts as a virtual dwelling, which implements detailed components to approximate a real building.

$$A(q)y(t) = B(q)u(t) + e(t) \tag{5.1}$$

where $A(q)$ and $B(q)$ are given by:

$$\begin{aligned} A(q) &= 1 + a_1 q^{-1} + ... + a_{n_a} q^{-n_a} \\ B(q) &= b_1 q^{-1-n_k} + ... + b_{n_b} q^{-n_b-n_k} \end{aligned} \tag{5.2}$$

where a_i and b_i are the model parameters, which are estimated with least squares identification. The time shift operator is defined as q. n_a and n_b are the orders of output $A(q)$, and input $B(q)$, respectively. The parameter n_k is the time delay between $y(t)$ and $u(t)$. Element $e(t)$ is a Gaussian white noise disturbance.

The ARX model is then converted to a discrete state-space model using MATLAB; the generic form of the model with p inputs, m outputs, and n state variables, is shown in Equation 5.3. The state-space model is the actual model which is used in the MPC, also referred to as *ARX-based model*. In order to translate the ARX model to state-space, the time delay is set to $n_k = 1$.

$$\begin{aligned} x(k + Ts) &= Ax(k) + Bu(k) \\ y(k) &= Cx(k) + Du(k) \end{aligned} \tag{5.3}$$

where Ts the sample time;
x is the $n \times 1$ state vector at time k;
y the $m \times 1$ output vector at time k;
u the $m \times 1$ input vector at time k;
A the $n \times n$ system matrix;
B the $n \times p$ input matrix;
C the $m \times n$ output matrix;
D the $m \times p$ feedthrough matrix.

In this work the model does not have direct feedthrough, therefore matrix D is a zero matrix.

5.1.1 System Identification

The ARX model is estimated by optimising the model parameters (a_i and b_i) with least squares identification, the objective of the optimisation routine is minimising the 1-step ahead prediction

error. Which is the difference between the predicted 1-step ahead temperature, and the actual temperature which can be found in real (simulation) data, as stated in Equation 5.4. This identification is available in MATLAB through the System Identification Toolbox. A disadvantage of this method is the possible inaccuracy of the multi-step ahead prediction. There are different approaches available in literature to overcome this problem, e.g. by using orthonormal basis filters [40]. However, this is currently not available in the MATLAB toolbox, and it is outside the scope of this work to implement this type of filters into MATLAB. Therefore it is not used in this thesis.

$$e(k) = y(k) - \hat{y}(k|k-1) \tag{5.4}$$

where $y(k)$ is the measured temperature at $t = k$, and $\hat{y}(k|k-1)$ is the predicted temperature at $t = k$ based on previous data up to $t = k - 1$. The data used in this thesis is generated by simulating the building with a simple PID-controller. An annual simulation to obtain identification data is executed with Dymola (Modelica), which is elaborated in the next paragraph.

5.1.2 Data Collection - System Identification

The input-output data used for the identification of the ARX model is collected by simulating the modelica house model. The HVAC-system is controlled by a simple (not optimised) PID-controller, which has a set point within the thermal comfort temperature band. The modelica model enables the use of data sets from different seasons, hence two weeks of every season are used to synthesise the ARX model. In this thesis an offline identification is executed, which means that the entire data set should be available during identification. For an adaptive approach, an online identification is necessary. The online approach will not be elaborated in this work; literature regarding this topic can be found in e.g. [24] [40]. The settings, and required variables used to execute the identification can be found in Table 5.1, and Table 5.2.

Table 5.1: System identification settings.

Type	**Setting**
Model order	Automatically chosen (see Chapter 6.1)
Sample time	900 [s]
Data collection periods	11 January - 26 January 12 April - 27 April 12 July - 27 July 11 October - 26 October

Table 5.2: Model variables.

Symbol	**Description**	**Unit**	**type**
Input variables			
T_{out}	Outdoor temperature	[K]	*Measured disturbance*
H_{solar}	Solar irradiance	[Wm^{-2}]	*Measured disturbance*
$\dot{Q}_{occupants}$	Occupant heat gain	[W]	*Measured disturbance*
$P_{heatpump}$	Consumed heat pump power	[W]	*Manipulated variable*
$\dot{Q}_{ventilation}$	Ventilation heat flux	[W]	*Manipulated variable*
$\dot{Q}_{solar}$	Solar heat gain	[W]	*Manipulated variable*
Output variable			
T_{room}	Room temperature	[K]	

5.2 Single Thermal Zone Building

The analysis is done in a single thermal zone building, the properties can be found in Table 5.3. The house is exposed to Dutch weather conditions (Amsterdam), and the construction properties are based on the reference buildings (EPC 0.4) of *Rijksdienst voor Ondernemend Nederland* [38]. The energy demand of the building is based on the calculation given by RVO, however the reference building contains 2.8 times more window surface per floor area than the designed building in this work. Nevertheless, this value will be used as a starting point for further comparisons. The dimensions, and the orientation of the dwelling are shown in Figure 5.1.

Table 5.3: Single thermal zone residential building (EPC 0.4) [38].

Property	**Value**
Floor surface	6×10.2 [m^2]
Ceiling surface	6×10.2 [m^2]
Window surface	5.6 [m^2]
Height	2.6 [m]
R_c Wall	4.5 [m^{2}K/W]
R_c Ceiling	6.0 [m^{2}K/W]
R_c Floor	3.5 [m^{2}K/W]
U Window	1.3 [W/m^{2}K]
Thermal capacity (within the insulated part)	29.5 [MJ/K]
HVAC energy demand of EPC-0.4 building	176 [MJ/m^2]

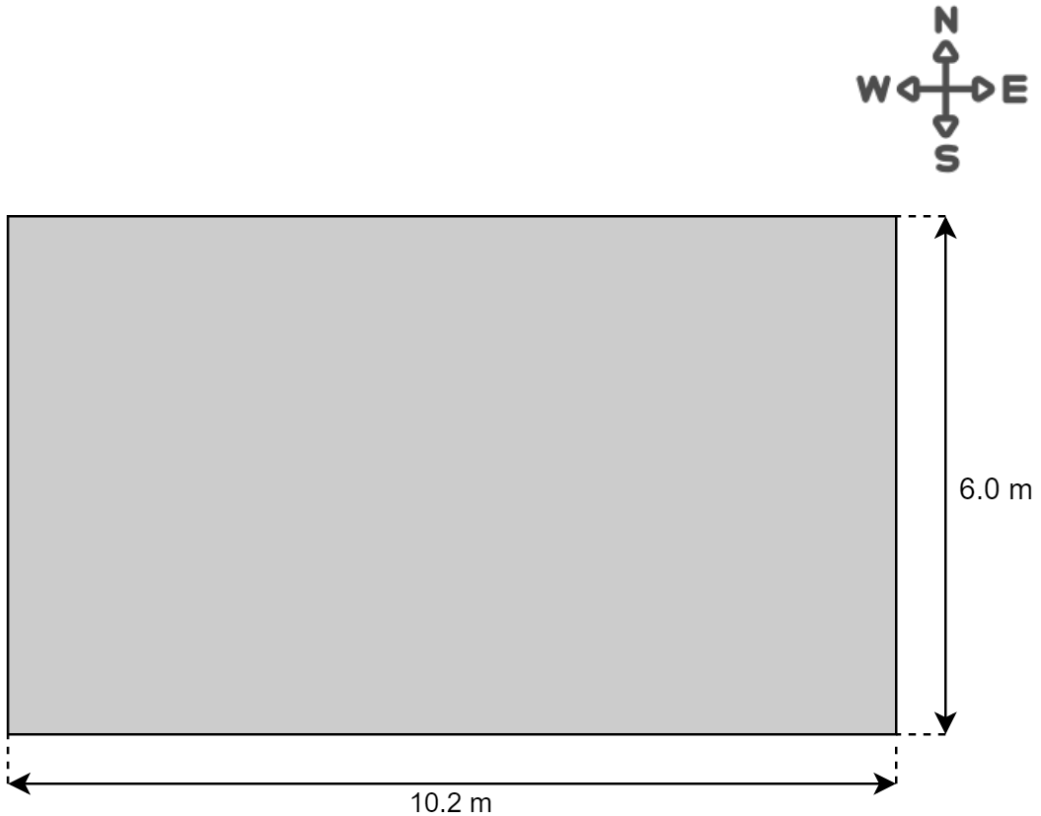

Figure 5.1: Dimensions and orientation of the building (top view).

The shading device, and the heat pump system are ideally controlled, by calculating the required shading and compressor factors (0-1) according to the setpoints, given by the outputs of the MPC ($\dot{Q}_{solar}$ & $P_{heatpump}$). The factors are computed with Equation 5.5 & 5.6.

$$y_{sha} = min\left(1,\ max\left(0,\ 1 - \frac{\dot{Q}_{solar} - \dot{Q}_{solar,min}}{\dot{Q}_{solar,max} - \dot{Q}_{solar,min}}\right)\right) \tag{5.5}$$

where $\dot{Q}_{solar}$ is the desired solar heat gain through the windows; $\dot{Q}_{solar,min/max}$ the minimum/maximum solar heat gain through the windows. Those values are calculated with the same model as implemented in the used thermal zone model, which is extracted from the Buildings library. Therefore, the modelled value is exactly the same value as is used in the artificial house. In order to compute $\dot{Q}_{solar,max}$, the solar shades are not used, so the total available irradiation can enter the building through the windows. $\dot{Q}_{solar,min}$ is calculated in the same manner, only with the shades down.

$$y_{heat\ pump} = \frac{P_{heatpump} \cdot COP_{nominal}}{\dot{Q}_{nominal}} \tag{5.6}$$

where $\dot{Q}_{nominal}$ is the nominal heating power of the heat pump when $P_{heatpump} = P_{max}$, and $COP_{nominal}$ is the Coefficient of Performance under nominal conditions.

This approach is chosen in order to separate the high level optimisation problem of the building, from the low level appliances control. Because the scope of this work is the high level problem, the control of appliances is made ideal within the computer simulation. Due to this approach each appliance can be integrated with its own control strategy in future research. The concept is visualised in Figure 5.2.

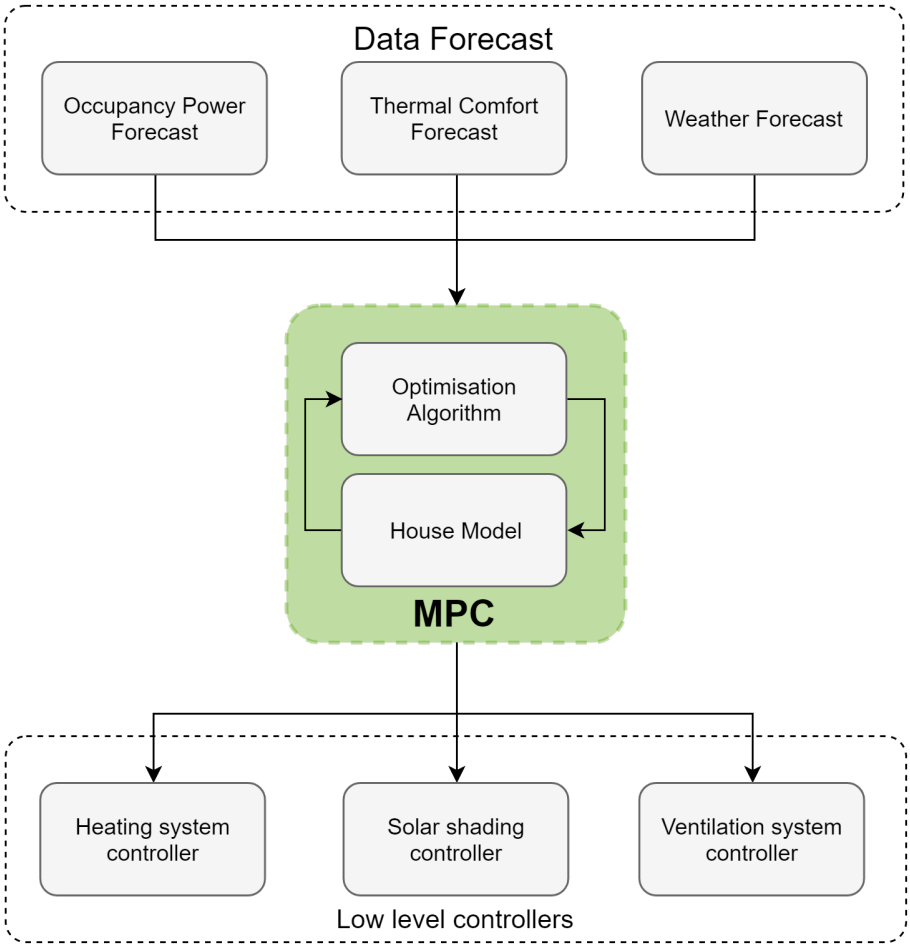

Figure 5.2: Visualisation of the controller hierarchy.

The properties required by the Modelica model of the heat pump based heating system are defined in Table 5.4. The radiator system is based on a low temperature heating system of Jaga [49]. The building is modelled, and simulated with the Modelica language within Dymola. Due to the large reusability of Modelica components the house model can be developed rather quickly, by using components of the Buildings library [37]. This virtual building will be used as replacement for a real house, this implies that the developed controller will be implemented, and analysed in this virtual house. The data-driven ARX model will be derived using simulation data obtained from this artificial house.

Table 5.4: Heating system for a single thermal zone residential building.

Property	**Value**
Heat pump type	Air-water
Maximum compressor power	625 [W]
Minimum work load	20 %
Nominal ΔT evaporator	-5 [K]
Nominal ΔT condenser	5 [K]
Nominal COP	4
Nominal supply temperature	35 [°C]
Nominal return temperature	30 [°C]
Nominal evaporator temperature	7 [°C]
Nominal condenser temperature	30 [°C]
Nominal ΔP evaporator	6000 [Pa]
Nominal ΔP condenser	600 [Pa]
Volume of expansion vessel	12 [l]
Floor heating	
Heating circuits	7
Pipes	PEX DN 25 (DIN 11850)
Area	6×10.2 [m^2]
Pipe distance	0.10 [m]
Radiator (EN 442.2)	
Type	Jaga: STRW.035 240 20
Maximum heating power	2500 [W]
Nominal ΔP	1000 [Pa]
Heat transfer exponent	0.15
Fraction radiant heat transfer	0.10
Mass of radiator	33 [kg]
Water volume of radiator	3.168 [l]

5.2.1 Model Structure

The single thermal zone building is modelled using the reusable modelica library of Berkeley University; *Buildings*. The building consists of four main components; a thermal zone model, a heating model, an occupancy model, and a natural ventilation model.

5.2.1.1 Thermal Zone Model

The thermal zone model is a mixed-air model, which assumes that the total air volume is mixed, and thus has a uniform temperature distribution. It can be connected to other thermal zones in order to create a multi-zone building. A comprehensive description of the thermal zone model can be found in Wetter et al. (2011) [41]. The relevant inputs of this model for the single zone case are the following:

- **uSha [-]**
  This is the control parameter (0-1) for the exterior solar shading devices. The set point given by the high level MPC will be ideally converted to a value between 0 (no shading) and 1 (full shading); this is further elaborated in Chapter 5.3.2.
- **q** [W/m^2]
  This is the internal heat gain due to occupancy, this value will be calculated by the occupancy model. The heat gain is divided into a radiative, convective, and latent component.
- **heaPorRad / heaPorAir (Radiator based heating system)**
  These two inputs are the radiative, and convective/conductive heat ports, respectively. These

are connected to the radiator of the heating system. A heat port is a modelica interface for one-dimensional heat transfer to provide algebraic coupling between (sub)models; the temperature [K], and the heat flow rate [W] are part of this interface.

- **surf_surfBou (Floor heating based heating system)**
  This heat port is connected to the floor heating system, which models the floor, and the floor heating system.
- **Fluid ports**
  The fluid ports are used to exchange air with the ventilation system.
- **Weather bus**
  This is an interface which connects the thermal zone to a weather file. This file contains among others properties like: temperature, solar radiation intensity, wind speed/direction, latitude, and air pressure.

Furthermore, construction parameters like wall material, thickness, and size can be set; the properties are chosen such that the building properties of Table 5.3 hold. Figure 5.3 shows the graphical representation of the model.

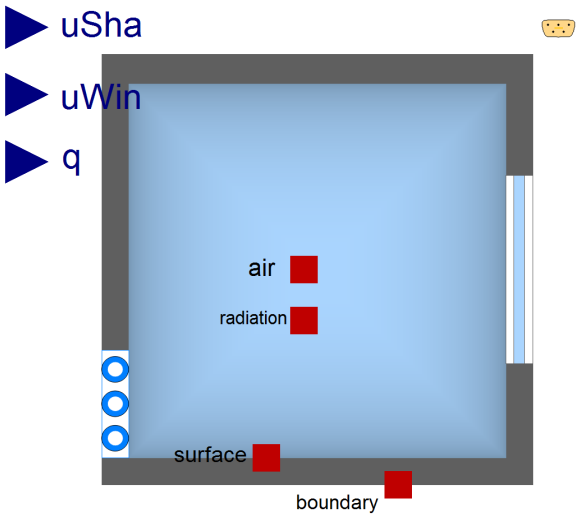

Figure 5.3: Visualisation of the reusable room model.

5.2.1.2 Heating System Model

The heating system block consists of several components of the same Buildings library [42], which are briefly stated here, and well documented in [42]. Note that in this study, the radiator and the floor heating system are not used at the same time.

- **Carnot heat pump**
  The heat pump is the heat source of the heating system, it is modelled as a heat pump whose coefficient of performance COP changes with temperatures in the same way as the Carnot efficiency changes.
- **Water pump**
  The pump is used to circulate the water from the heat pump to the radiator and back.
- **Fan**
  The fan is used to force cool, ambient air over the condenser of the heat pump.
- **Radiator**
  The radiator model models the thermal heat gain from the hot water to the room air. The model is based on the European norm EN442.2, which is used by manufacturers of radiators.
- **Parallel circuit slab**

This component models the floor heating system, it replaces the total floor model of the thermal zone model (Room). Figure 5.4 shows the thermal resistance network of the model. Where *con_a* computes transient heat conduction between heat port *surf_a* and the fictitious plane between *concrete* and *insulation*. The pipes of the floor heating system are located inside this plane. Note that a fictitious plane does not physically exist, it is solely used for modelling purposes. Construction *con_b* models the transient heat conduction between the plane and heat port *surf_b*. The heat ports *surf_a* and *surf_b* are connected with the room model, and soil model, respectively. Note that the number of layers, and material of each layer can be modified within Modelica. The figure is only a visualisation of the floor heating model.

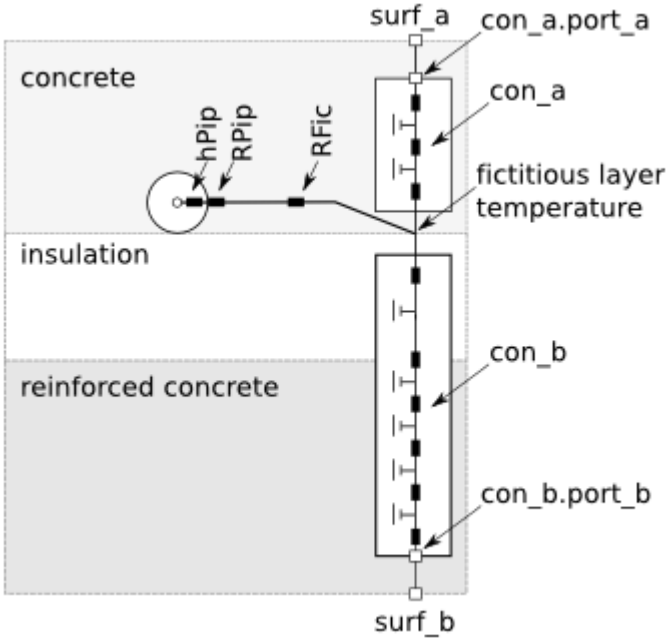

Figure 5.4: Thermal resistance network of the floor heating system [42].

- **Expansion vessel**
  The expansion vessel accounts for the thermal expansion of the water inside the closed system.

5.2.1.3 Natural Ventilation Model

The natural ventilation block consists again of some components of the Buildings library [42]:

- **Orifice**
  This component is used to model an opening in the wall, like a vent.
- **Valve**
  The valve is used to close, or to open the vent. The opening is variable from 0-100%.
- **Mass flow sensor**
  Because the amount of natural ventilation cannot be controlled ideally, this sensor is used to acquire feedback from the ventilation system; which is used by a PI-controller.
- **Volume**
  This component acts as the ambient air, the model variables are obtained from the weather file.

Important parameters used for the simulation are given in Table 5.5. The surface values are chosen in order to meet the minimum ventilation rate, which is required by Dutch legislation (NEN 1087,

2007) [43] [12]. The model lumps the total ventilation area to two vents (bottom and top).

Table 5.5: Natural ventilation system for a single zone residential building.

Property	**Value**
Minimum ventilation rate	0.9 [l/sm^2]
Height position of top vent	2.6 [m]
Height position of bottom vent	0 [m]
Surface of top vent	1.3 [m^2]
Surface of bottom vent	1.3 [m^2]

5.2.1.4 Occupancy Model

The occupancy model is a custom model which calculates the total heat gain produced by, and due to actions of occupants. A text file contains the number of occupants at a certain moment in a certain room type. An occupancy profile of Alders (2016) [6] is used for this model, the profile can be found in Appendix A. The bed room type uses a different average heat gain value per m^2. This accounts for the different appliances, and activities in the room; the used heat gains are stated in Table 5.6. These heat gains are split into a radiative, convective, and latent component, which is defined in Table 5.7.

Occupancy modelling is an ongoing research topic, and future improvements can be implemented in this system due to the hierarchical approach. In this study is chosen for a rather simple model, e.g. occupant heat gain is not coupled to metabolic levels of occupants. Moreover, the heat gain fractions are in reality different for each single appliance. Whereas for this work reasonable heat gains are already sufficient, rather than highly detailed values. Because the occupancy heat gain is an input variable of the prediction model, which is trained with comparable values, and it is an input of the virtual dwelling itself. This implies that the occupancy model should be more detailed for real applications, in order to give an accurate estimate of the upcoming future occupancy heat gains.

Table 5.6: Heat gain values due to occupancy.

Property	**Occupied**	**unoccupied**
$\dot{Q}_{person}$	75 [W/person]	-
$\dot{Q}_{appliances,\ bedroom}$	1 [W/m$^2_{\text{floor area}}$]	0 [W/m$^2_{\text{floor area}}$]
$\dot{Q}_{appliances,\ bathroom}$	10 [W/m$^2_{\text{floor area}}$]	1 [W/m$^2_{\text{floor area}}$]
$\dot{Q}_{appliances,\ livingroom}$	10 [W/m$^2_{\text{floor area}}$]	1 [W/m$^2_{\text{floor area}}$]
$\dot{Q}_{appliances,\ kitchen}$	10 [W/m$^2_{\text{floor area}}$]	1 [W/m$^2_{\text{floor area}}$]

Table 5.7: Radiative, convective, and latent heat fractions.

Type	**Value**
Radiative	0.26
Convective	0.52
Latent	0.22

5.2.1.5 Model Overview

All components are coupled in order to model the dwelling. In addition, a noise generator ($\mu = 0$, $\sigma = 0.1$) is added to the operative temperature sensor to account for measurement inaccuracies. This gave a better estimation result by the ARX identification, due to additional excitation in

the signal. This results in a dwelling with one thermal zone. However, in order to calculate the internal heat gains, and the comfort temperature, the dwelling is divided into two rooms, which are modelled as one single thermal zone, see Table 5.8. The area of each room type, and the number of occupants in the room type, is used as a weighting value to compute the single zone comfort temperature (weighted average), as shown in Equation 5.7.

$$\begin{aligned} w_j &= A_j \cdot \rho_j \\ T_{comfort,\,max} &= \frac{\sum_j T_{comfort,\,j,\,max} \cdot w_j}{\sum_j w_j} \\ T_{comfort,\,min} &= \frac{\sum_j T_{comfort,\,j,\,min} \cdot w_j}{\sum_j w_j} \\ \rho &\in \mathbb{N} \\ j &\in \{other\ room,\ bed\ room\} \end{aligned} \tag{5.7}$$

where w is the weight factor, ρ is the number of occupants in the specific room type, A the surface area of the room type, and j the room type specifier.

The bath room did not get a separate group, because the comfort temperature was not useful when switching from bed room to bath room. In that case, the lower comfort bound is higher than the upper comfort bound of the previous time step. This inevitably results in a temperature violation, which distorts the controller performance analysis. Moreover, generally the time spend in bath rooms is low. Using a single thermal zone is a simplification of reality, where every room can have another temperature. In order to model the temperature per zone, multiple thermal zone models should be implemented, and coupled with each other. The Modelica model of the artificial house is visualised in Figure 5.5.

Table 5.8: Modelled room types.

Modelled room type	**Occupancy room type used in Alders (2016) [6]**	**Thermal comfort room type**	**Area**
Other rooms	Living room Bath room Kitchen	Other rooms Bath room	$0.72 \cdot A_{floor,\,total}$
Bed room	Bed room	Bed room	$0.28 \cdot A_{floor,\,total}$

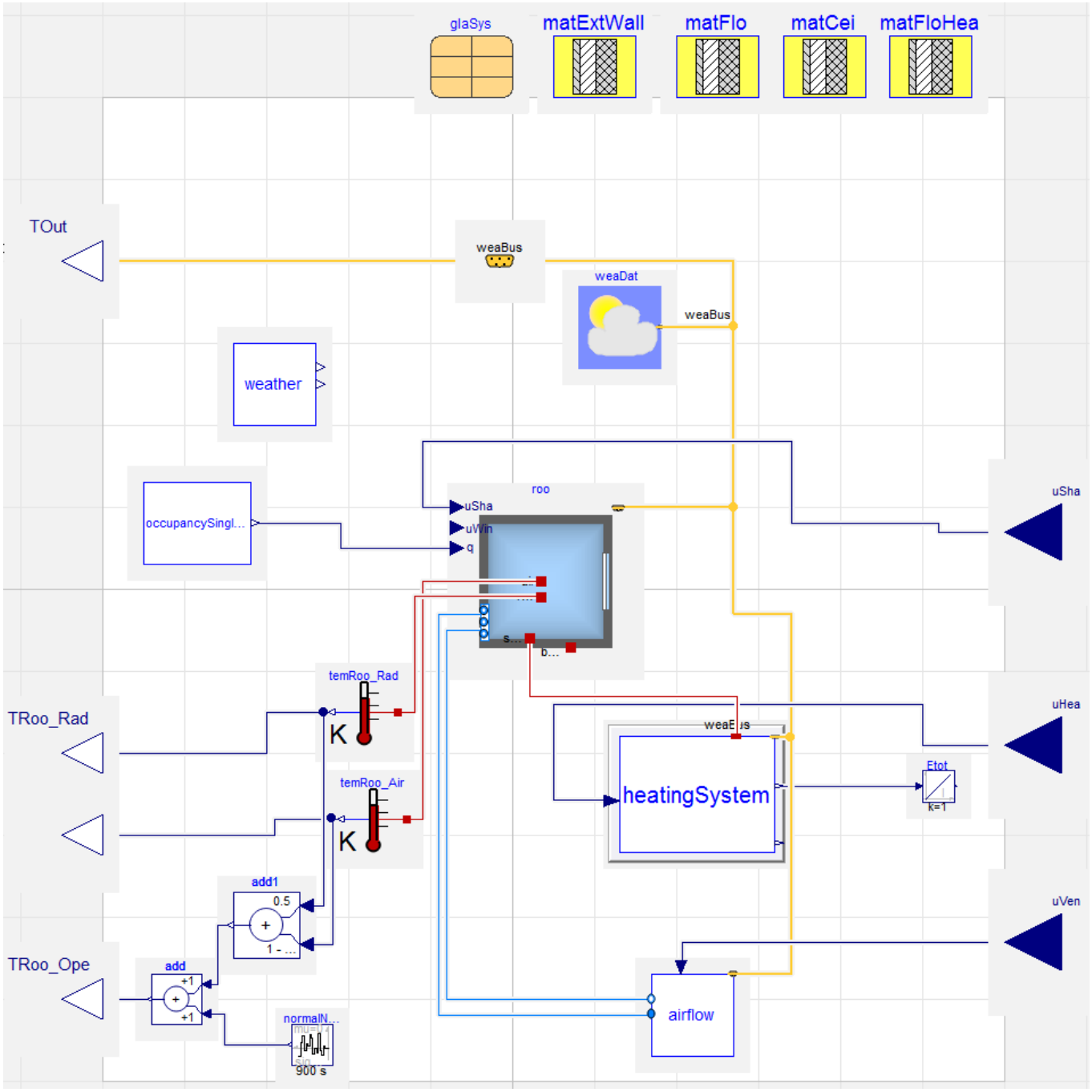

Figure 5.5: Virtual house model, with a floor heating system.

5.2.2 Simple HVAC PID-controller

In order to collect the closed-loop data set for the offline system identification process, two simple (non optimised) P(ID)-controllers are designed. One for the heating system, and one for the natural ventilation system. The properties, and set-points of the controllers are given in Table 5.9, and Figure 5.6, respectively. The solar shading is coupled to a pulse generator, so that the shades are either opened or closed. The pulse generator has a period of 50400 seconds (14 hours), the pulse is 1 50% of the time. This results in highly varying solar excitation during the identification period, which results in better identification data.

Table 5.9: Simple P(ID) controllers for a single zone residential building.

Properties controller	**Values heating system**	**Values ventilation system**
Gain	70	1
Time constant of integrator	13902 [s]	-
Time constant of derivator	3476 [s]	-
Upper limit of output	625 [W]	0.05 [kg/s]
Lower limit of output	0 [W]	0.007 [kg/s]

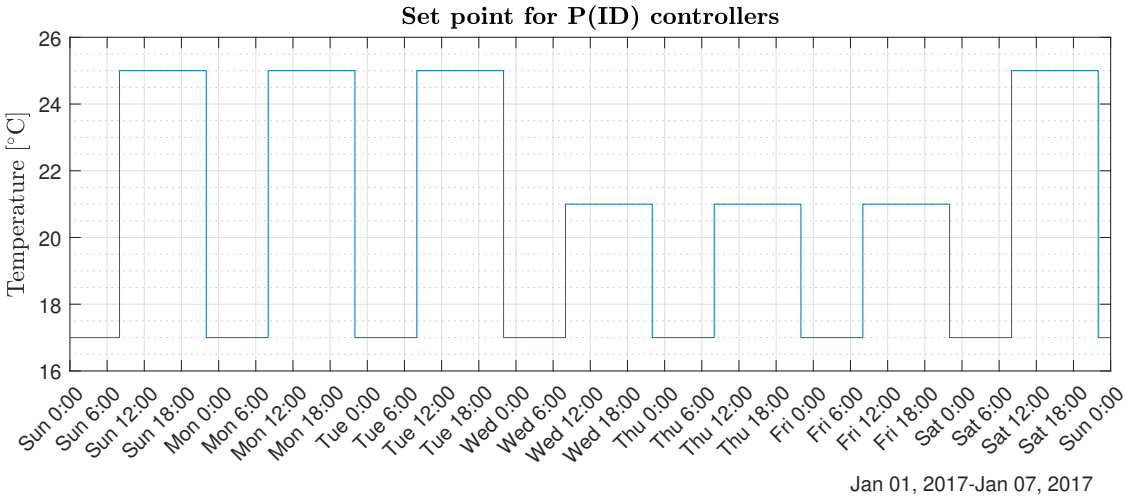

Figure 5.6: Set points for the P(ID)-controllers during identification.

5.3 Economic Model Predictive Control

Model predictive control (MPC) can handle large, multi-variable systems, which are subject to hard constraints on states and inputs [44]. A conventional MPC solves a finite-horizon optimal control problem in a receding horizon fashion, by minimizing quadratic cost functions [45]. This cost function tries to move the plant to optimal steady-state conditions, which is accomplished by choosing the stage cost to be minimal at the optimal pair of steady state and input [44]. Nonetheless, this does not necessarily lead to optimal economic conditions, which is often desired in systems, as well as in the Thermal Comfort System. In order to achieve optimal economic conditions, the quadratic objective is transformed in an economic objective. This economic MPC optimizes directly the economic performance of the system, rather then tracking a setpoint [44]. An economic algorithm of this type might result in non-converging behaviour of the closed-loop system.

The controller will be designed in MATLAB by using the YALMIP optimization toolbox [46]. One of the challenges of designing an economic MPC is developing a proper objective function. This objective should minimize the energy costs, while maintaining thermal comfort. On the other hand, thermal comfort criteria can be implemented within optimisation constraints instead. This allows an upper and a lower temperature boundary, and gives the controller freedom to minimize energy costs within the thermal comfort zone. For the case of a thermal comfort system, the economic operating costs consists mainly of the power consumed by the compressor of the heat pump. The power consumed by solar shading and the (natural) ventilation system is small in comparison with the heat pump. Therefore, this energy consumption is neglected in this analysis. Chapter 5.3.1 will elaborate on this topic.

The control variables of the MPC are; the compressor power, the solar gain through windows, and the mass flow of the (natural) ventilation system. The controller uses the internal building model to stay within the thermal comfort zone, by predicting the temperature response in the near future. This internal building model is an ARX model, which is converted to a discrete state-space representation, see Equation 5.3.

5.3.1 Optimisation Algorithm

Each time step the MPC executes an optimisation cycle over the entire horizon, in order to obtain the optimal control values. The optimisation problem is formulated by defining a cost function (objective), and by constraining the decision variables. The solver calculates the optimal decision variables by minimizing the objective. It is advised to define a linear objective as well as linear constraints, in order to reduce computational time, and to avoid infeasible models. The initial optimisation problem is defined in Equation 5.8.

$$\begin{aligned} \min \quad & \sum_{t=1}^{Horizon} P_{heatpump}(t) \\ \text{s.t.} \quad & T_{room} \in [T_{comfort,min}, T_{comfort,max}] \\ & P_{heatpump} \in 0 \cup [0.2 \cdot P_{heatpump,max}, P_{heatpump,max}] \\ & \dot{m}_{ventilation} \in [\dot{m}_{ventilation,min}, \dot{m}_{ventilation,max}] \\ & \dot{Q}_{solar} \in [\dot{Q}_{solar,min}, \dot{Q}_{solar,max}] \end{aligned} \tag{5.8}$$

However, the ARX-model, as defined in Table 5.1, does not accept $\dot{m}_{ventilation}$ as an input variable. While this variable is convenient to constrain, due to legal requirements; see Table 5.5. Therefore, the mass flow rate is internally converted to $\dot{Q}_{ventilation}$, using Equation 5.9.

$$\dot{Q} = \dot{m} c_{p,air} \Delta T \tag{5.9}$$

where $\dot{m}$ is the mass flow rate entering the dwelling in kg/s; $c_{p,air}$ the specific heat coefficient of air in J/kgK; ΔT the difference between indoor and outdoor temperature.

5.3.1.1 Soft Constraints

The optimisation problem as defined in Equation 5.8 only contains hard constraints. When the solver cannot find a solution within this type of constraint, the problem is infeasible, and the results are useless. Infeasibility often occurs when the output of the internal prediction model is hard constrained. The solver can only alter the output by modifying input variables. However, there is no input combination possible inside the constrained area. By introducing soft constraints in the optimisation model, this problem is eliminated. In order to convert a hard constraint into a soft constraint, an additional slack variable is added to the (in)equality constraint; the slack variable is then added to the objective. Equation 5.10 shows the modification of the optimisation problem as stated in Equation 5.8. The weighting value (ψ) of the slack variable is chosen to be large ($1e5$), in order to penalise small violations of the temperature boundaries.

$$\begin{array}{lrcl} \min & \sum_{t=1}^{Horizon} & P_{heatpump}(t) + \psi_{comfort} \cdot S_{comfort}(t) & \\ \text{s.t.} & T_{room} & \in & [T_{comfort,min} - S_{comfort}, T_{comfort,max} + S_{comfort}] \\ & S_{comfort} & \geq & 0 \end{array} \tag{5.10}$$

5.3.1.2 Ventilation - McCormick's Envelope

From a heating/cooling perspective, ventilation is mainly used for cooling. After all, the outdoor temperature is most of the time lower than the indoor temperature. In some occasions (when the outdoor temperature is higher than the indoor temperature) ventilation can be used for heating; as can be derived from Equation 5.9. The optimisation algorithm determines which mode is required. However, Equation 5.9 induces a bi-linear problem, which is computationally expensive and often leads to infeasible problems. In order to cancel the bi-linearity, McCormick's envelope is used. This is a convex relaxation to approximate the desired variable, on a convex (non)linear manner [47]. The application, as proposed in this work, results in a convex linear problem. The constraints given in Equation 5.11 are an extension of the original optimisation problem stated in Equation 5.8.

$$\begin{array}{lrcl} \min & \sum_{t=1}^{Horizon} & P_{heatpump}(t) + S_{ventilation}(t) & \\ \text{s.t.} & \Delta T & \in & [\Delta T_{min}, \Delta T_{max}] \\ & w & \geq & \Delta T_{min}\dot{m}_{ventilation} + \Delta T\dot{m}_{ventilation,min} - \Delta T_{min}\dot{m}_{ventilation,min} \\ & w & \geq & \Delta T_{max}\dot{m}_{ventilation} + \Delta T\dot{m}_{ventilation,max} - \Delta T_{max}\dot{m}_{ventilation,max} \\ & w & \leq & \Delta T_{max}\dot{m}_{ventilation} + \Delta T\dot{m}_{ventilation,min} - \Delta T_{max}\dot{m}_{ventilation,min} \\ & w & \leq & \Delta T_{min}\dot{m}_{ventilation} + \Delta T\dot{m}_{ventilation,max} - \Delta T_{min}\dot{m}_{ventilation,max} \\ & S_{ventilation} & \in & [S_{ventilation,min}, S_{ventilation,max}] \\ & \dot{Q}_{ventilation} & = & c_p w \\ & \dot{Q}_{ventilation} & \in & [\dot{Q}_{ventilation,min}, \dot{Q}_{ventilation,max}] \\ & \neg coolingMode & \implies & \dot{Q}_{ventilation} = -S_{ventilation} \\ & coolingMode & \implies & \dot{Q}_{ventilation} = S_{ventilation} \end{array} \tag{5.11}$$

The slack variable $S_{ventilation}$ introduced in Equation 5.11 is added to the objective function; the objective is minimised by the solver, so is the slack variable. This results in maximising $\dot{Q}_{ventilation}$ while not in cooling mode, and minimising $\dot{Q}_{ventilation}$ while in cooling mode. Note that the slack variable is only introduced to enable the algorithm to add or remove the minus sign

from the $\dot{Q}_{ventilation}$, regarding the system's mode. If there is no cooling mode option required, $-\dot{Q}_{ventilation}$ can be added to the objective directly. The minimum and maximum values of $S_{ventilation}$ and $\dot{Q}_{ventilation}$ depend on the ventilation system of the dwelling, and should be configured accordingly, before the optimisation cycle starts. Every three hours the system's mode is determined, and is constant during the optimisation cycle; see Chapter 5.3.1.5. Furthermore, some other variables are introduced, which will be explained here. Equation 5.9 can be rewritten as:

$$\begin{aligned} w &= \dot{m}\Delta T \\ \dot{Q} &= c_p w \end{aligned} \tag{5.12}$$

The bounds on ΔT are first computed through a simpler optimisation problem, namely by running the problem with fixed ventilation mass flow rates (minimal and maximal). Then the bounds are sent to the second stage as parameters, which is elaborated in Chapter 5.3.1.6. This implies that two additional optimisation cycles are necessary, in order to compute the final result.

5.3.1.3 Solar Shading

Solar shading is used to control the amount of solar irradiation entering the building. Hence, it can be used to heat the building when there is solar irradiation available, or block incoming irradiation when no heat is required. In order to control the solar shading system properly, the following constraints are added to the original optimisation problem defined in Equation 5.8.

$$\begin{aligned} \min \quad & \sum_{t=1}^{Horizon} P_{heatpump}(t) + S_{solar}(t) \\ \text{s.t.} \quad & S_{solar} \in [0, \dot{Q}_{solar,\,max}] \\ coolingMode \implies & \dot{Q}_{solar} = \dot{Q}_{solar,\,min} + S_{solar} \\ \neg coolingMode \implies & \dot{Q}_{solar} = \dot{Q}_{solar,\,max} - S_{solar} \end{aligned} \tag{5.13}$$

5.3.1.4 Stabilising Control Actions

The optimisation algorithm's main concern is minimising the objective, while staying within the defined constraints. This may lead to highly fluctuating control actions, which is not desirable. In order to limit highly fluctuating control actions, the rate of change can be penalised; by adding this rate to the cost function. Consequently, the optimisation problem becomes computationally more complex. However, due to the large time step (15 minutes) of the developed controller, fluctuating control actions regarding solar shading are not regarded important in this work. Hence, this is not implemented in the current algorithm. On the other hand, fluctuating control actions related to the heat pump are penalised in order to prevent start-stop behaviour. Like in Chapter 5.3.1.1, a slack variable is used to tackle this problem. Equation 5.14 shows the implementation of the new constraint. The weighting factor ψ is chosen to be small, namely $\psi = 2$ for floor heating, and $\psi = 40$ for radiator heating. The weighting value for radiator heating is larger, to prevent high fluctuating temperature response. Some trial and error tuning was performed to determine these values.

$$\begin{aligned} \min \quad & \sum_{t=1}^{Horizon} P_{heatpump}(t) + \psi_{\Delta heatpump} \cdot S_{\Delta heatpump}(t) \\ \text{s.t.} \quad & \Delta P_{heatpump} \in [-S_{\Delta heatpump}, S_{\Delta heatpump}] \\ & S_{\Delta heatpump} \geq 0 \end{aligned} \tag{5.14}$$

5.3.1.5 Cooling Mode

Every three hours the controller determines its mode, by computing the evolution of T_{room}. This prediction is computed by using the *ARX-based* model, in which the heat pump is turned off, the

solar shades are open, and the ventilation is set to minimal. The method to determine the system's mode is given in Algorithm 1. The used scalar values can be altered to prevent overheating.

Algorithm 1: Algorithm to determine if cooling mode should be enabled

Data: $\mathsf{HP}_{\text{on, history}}$ is a boolean which is set to true, when the heat pump was enabled in the past 24 hours.
`nnz()` calculates the number of non-zero elements.
steps is the total amount of time steps since start, each time step represents a period of 15 minutes.
Result: coolingMode is a boolean value, which is sent to the optimisation cycle as a parameter.
input : $T_{comfort,\,min}$, $T_{comfort,\,max}$, $\dot{m}_{ventilation,\,min}$, $\dot{Q}_{solar,\,max}$, $\mathsf{HP}_{\text{on, history}}$
output: coolingMode
begin
  if `mod(`*steps, 12*`) ==` *1* **then**
    $T_{room} \leftarrow$ `getTRoom(`$P_{heatpump}$, $\dot{m}_{ventilation}$, $\dot{Q}_{solar}$`)`
    if $T_{comfort,\,max} \leq T_{room}$ **and** $\mathsf{HP}_{\text{on, history}}$ **then**
      if `nnz(`$T_{room} \geq (T_{comfort,\,max} - (T_{comfort,\,max} - T_{comfort,\,min}) * 0.05 \geq 10$`)` **then**
        coolingMode := true
      else
        coolingMode := false
    else
      coolingMode := false

5.3.1.6 Reducing Computing Time

The computing power required to solve an optimisation problem increases with complexity of the problem. For this work annual simulation data is required. Therefore, the computing time for each optimisation cycle should be minimised. The solution used in this thesis is reduction of decision variables. In order to achieve this, at first the ventilation rate is fixed to a single value (minimum ventilation). This decision is based on minimising heat loss by ventilation, because outdoor temperature is normally lower than indoor temperature. The optimisation problem is solved, which results in control actions and a temperature evolution forecast. If the predicted maximum room temperature is below the upper comfort temperature bound during the entire horizon (24 hours), and the outdoor temperature is lower than the room temperature, then the computed control actions are used. If one of the previous conditions does not hold, then the temperature evolution with maximum ventilation is calculated. This is then inserted as temperature boundary in the original optimisation problem, to compute all optimal control actions (ventilation, solar shading, and heat pump power). Therefore, only one single optimisation cycle is processed if sufficient, instead of three; yielding the same result. The psuedo-code representation of the algorithm is given in Algorithm 2.

Algorithm 2: Time reduction algorithm

Data: MPC inputs not relevant to this part of the code are omitted for clarity.
`MPC()` is the controller which implements the optimisation cycle.
Result: Control actions for the low level appliance controllers.
input : coolingMode (boolean)
output: $\{P_{heatpump}, \dot{m}_{ventilation}, \dot{Q}_{solar}\}$
begin
  $\{T_{room,\ min.\ ventilation}, P_{heatpump}, \dot{m}_{ventilation}, \dot{Q}_{solar}\} \leftarrow$ `MPC(`$\dot{m}_{ventilation,\ min}$, *coolingMode*`)`
  if $T_{room,\ min.\ ventilation} < T_{comfort,\ max}$ **and** $T_{room,\ min.\ ventilation} > T_{out}$ **then**
    return $\{P_{heatpump}, \dot{m}_{ventilation}, \dot{Q}_{solar}\}$
  else
    $\{T_{room,\ max.\ ventilation}, P_{heatpump}, \dot{m}_{ventilation}, \dot{Q}_{solar}\} \leftarrow$ `MPC(`$\dot{m}_{ventilation,\ max}$, *coolingMode*`)`
    $dT1 \coloneqq T_{out} - T_{room,\ min.\ ventilation}$
    $dT2 \coloneqq T_{out} - T_{room,\ max.\ ventilation}$
    $dT_{min} \coloneqq$ `min` $(dT1,\ dT2)$
    $dT_{max} \coloneqq$ `max` $(dT1,\ dT2)$
    $\{P_{heatpump}, \dot{m}_{ventilation}, \dot{Q}_{solar}\} \leftarrow$ `MPC` $(dT_{min},\ dT_{max},$ coolingMode$)$
    return $\{P_{heatpump}, \dot{m}_{ventilation}, \dot{Q}_{solar}\}$

5.3.1.7 Final Optimisation Problem Definition

The final optimisation problem is obtained by compiling all extensions (Equation 5.8 5.10 5.11 5.13 5.14) discussed in previous paragraphs into one formulation, see Equation 5.15.

$$
\begin{aligned}
\texttt{min} \quad & \sum_{t=1}^{Horizon} P_{heatpump}(t) + 100000 \cdot S_{comfort}(t) + S_{ventilation}(t) + S_{solar}(t) + \\
& \qquad\qquad\qquad\qquad\qquad\qquad\qquad\qquad\qquad\qquad 2 \cdot S_{\Delta heatpump}(t) \\
\text{s.t.} \quad & T_{room} \in [T_{comfort,min} - S_{comfort}, T_{comfort,max} + S_{comfort}] \\
& S_{comfort} \geq 0 \\
& P_{heatpump} \in 0 \cup [0.2 \cdot P_{heatpump,max}, P_{heatpump,max}] \\
& \dot{m}_{ventilation} \in [\dot{m}_{ventilation,min}, \dot{m}_{ventilation,max}] \\
& \dot{Q}_{solar} \in [\dot{Q}_{solar,min}, \dot{Q}_{solar,max}] \\
& \Delta T \in [\Delta T_{min}, \Delta T_{max}] \\
& w \geq \Delta T_{min}\dot{m}_{ventilation} + \Delta T\dot{m}_{ventilation,min} - \Delta T_{min}\dot{m}_{ventilation,min} \\
& w \geq \Delta T_{max}\dot{m}_{ventilation} + \Delta T\dot{m}_{ventilation,max} - \Delta T_{max}\dot{m}_{ventilation,max} \\
& w \leq \Delta T_{max}\dot{m}_{ventilation} + \Delta T\dot{m}_{ventilation,min} - \Delta T_{max}\dot{m}_{ventilation,min} \\
& w \leq \Delta T_{min}\dot{m}_{ventilation} + \Delta T\dot{m}_{ventilation,max} - \Delta T_{min}\dot{m}_{ventilation,max} \\
& S_{ventilation} \in [S_{ventilation,min}, S_{ventilation,max}] \\
& \dot{Q}_{ventilation} = c_p \cdot w \\
& \dot{Q}_{ventilation} \in [\dot{Q}_{ventilation,min}, \dot{Q}_{ventilation,max}] \\
& \Delta P_{heatpump} \in [-S_{\Delta heatpump}, S_{\Delta heatpump}] \\
& S_{\Delta heatpump} \geq 0 \\
& S_{solar} \in [0, \dot{Q}_{solar,max}] \\
\neg coolingMode \implies & \dot{Q}_{ventilation} = -S_{ventilation} \\
\neg coolingMode \implies & \dot{Q}_{solar} = \dot{Q}_{solar,max} - S_{solar} \\
coolingMode \implies & \dot{Q}_{ventilation} = S_{ventilation} \\
coolingMode \implies & \dot{Q}_{solar} = \dot{Q}_{solar,min} + S_{solar}
\end{aligned}
\tag{5.15}
$$

YALMIP is used to convert this optimisation problem into a set which can be read by the GUROBI solver [48]; a free academic license is available for this solver. In addition, YALMIP handles all communication with GUROBI, and can be used within a simulink model. This enables developers to implement, and simulate the developed algorithm in a straight-forward manner. The developed Simulink model is elaborated in Chapter 5.4.

5.3.2 Handling Optimisation Results

The variables computed by the optimisation algorithm cannot be used by the HVAC system model directly, due to the design of those (external) models. The input for the heat pump is a factor with bounds [0,1]. The factor is calculated by Equation 5.6. The shading factor, which is an input of the thermal zone model, with bounds [0,1] is computed with Equation 5.5. The optimal mass flow rate $\dot{m}_{ventilation}$ for the ventilation system is sent to a PI-controller; which controls a valve so that the mass flow rate is equal to the set point.

5.4 Simulink

The economic MPC designed in Chapter 5.3 is implemented in Simulink via an *Interpreted MATLAB Function*-block. All inputs required by the MPC function can be connected to outputs of other Simulink blocks. The main blocks in the developed Simulink model are:

- **Artificial house (FMU)**
  This block implements the Modelica model as described in Chapter 5.2. This block is a replacement for a real house, which enables developers, and researchers to quickly test new/modified algorithms or solutions. Moreover, different HVAC systems can be implemented in existing building models, without the need to start from scratch. By using the Functional Mock-up Interface standard, Modelica models and Simulink models can be coupled, as explained in Chapter 3.4. The FMU uses internally the CVODE solver, which is currently the only applicable solver in Dymola, without additional licenses.
- **MPC block (Interpreted MATLAB Function)**
  The block calls a MATLAB function which implements the optimisation algorithm developed in Chapter 5.3.1. The control variables are exported to the artificial house.
- **Kalman filter**
  The Kalman filter block is available in the Control Systems Toolbox. The filter is used to observe the states of the internal MPC model (ARX-based model). These states are required to forecast the future temperature evolution of the building. The settings of the filter are shown in Table 5.10. These settings are guessed values, which give acceptable results; hence further optimisation of the kalman filter was not included in the scope of this work.
- **Weather block**
  The weather block reads weather information on a quarterly scale, according to the TMY3 (Typical Meteorological Year) standard. Extensive (free) weather data can be found at `https://energyplus.net/weather`.

Table 5.10: Kalman filter settings.

Setting	**Value**
System Model	ARX-based state space model (Chapter 5.1)
Q	1
R	1
N	0

The communication step size of the FMU is 900 seconds, which is equal to the sample time of the MPC. Furthermore, a variable-step solver is used in the simulink model. The FMU contains the Sundials CVODE solver, which is the default setting of Dymola. The solver settings are given in Table 5.11.

Table 5.11: Simulink solver settings.

Setting	**Value**
Type	Variable-step
Solver	auto (VariableStepDiscrete)
Max step size	auto (900)
Relative tolerance	default (1e-7)

Chapter 6: Results

This chapter presents the performance analysis of the developed MPC controller. First, various scenarios are developed to assess the performance in different circumstances, these are defined in Table 6.1. Scenario 8 consist of multiple simulations with different disturbance resolutions. Second, the identification results of the internal prediction model are given. Third, in order to assess the quality of the system, several performance indicators are defined. Finally, an in-depth analysis of all scenarios is presented.

Table 6.1: Analysis scenarios

	Floor heating	**Radiator**	**Window orientation**	**Original thermal comfort model**	**Uncertainty in measured disturbances**
Scenario 1	Yes	No	South façade	Yes	No
Scenario 2	No	Yes	South façade	Yes	No
Scenario 3	Yes	No	North façade	Yes	No
Scenario 4	Yes	No	East façade	Yes	No
Scenario 5	Yes	No	West façade	Yes	No
Scenario 6	Yes	No	South façade	Yes, with offsets	No
Scenario 7	No	Yes	South façade	Yes, with offsets	No
Scenario 8	Yes	No	South façade	Yes	Yes (Resolution: 1, 3, 6 hours)

6.1 System Identification

This section shows the results of the ARX system identification for all used models. The model orders shown in Table 6.2 are acquired using the Matlab function *selstruct*; this function selects the best orders based on the Akaike information criterion (AIC) [50]. The AIC is used to estimate the likelihood of a model to predict future values, the model with the lowest AIC is expected to be the best model. In addition, in Table 6.2 the prediction accuracy of the used models is shown. The fit is obtained by comparing prediction values with actual validation data, using Equation 6.1. The models with a floor heating system tend to perform quite well at long forecast horizons, while the model with a radiator heating system performs bad on average; the 1-step ahead forecast is good for all models.

$$\text{fit} = (1 - \frac{\|y - \hat{y}\|}{\|y - mean(y)\|}) * 100\% \tag{6.1}$$

where y is validation data output, and $\hat{y}$ is the output of the ARX model.

Table 6.2: Model orders, and prediction accuracy of identified ARX models.

Model	$\mathbf{n_a}$	$\mathbf{n_b}$	**1-step ahead fit**	**Average 1-96 step ahead fit**
Window orientation: South	7	[3 5 7 6 8 8]	90.2%	76.3%
Window orientation: North	7	[3 6 8 7 8 8]	90.1%	76.5%
Window orientation: East	7	[3 5 8 5 8 8]	89.8%	75.3%
Window orientation: West	7	[3 5 8 7 8 8]	90.2%	76.4%
Radiator Heating System	8	[3 4 7 8 8 8]	87.5%	36.1%

6.2 Performance Indicators

The performance of the MPC is assessed by simulating a full year scenario. Important performance indicators for the analysis are: undercooling time, overheating time, energy usage, flexibility regarding different window orientation, and the influence of uncertain disturbance variables. Undercooling is defined as the state of having an operational temperature below the lower thermal comfort boundary. The building is overheated when the operational temperature is higher than the upper thermal comfort bound. The thermal comfort bounds are calculated by the model described in Chapter 2.2.1. The undercooling, and overheating time are bundled into a Key Performance Indicator (KPI); the discomfort index I_d [°Ch], which is defined as the sum of all temperature violations, is shown in Equation 6.2. Note that the used PPD for thermal discomfort is 10%, which is assumed to be acceptable, see Chapter 2.2.1.

$$\begin{aligned} I_{d,\,cool} &= \int_{t=0}^{1\ year} \texttt{min}\big\{0, T_{room}(t) - T_{comfort,\,min}(t)\big\}dt \\ I_{d,\,heat} &= \int_{t=0}^{1\ year} \texttt{max}\big\{0, T_{room}(t) - T_{comfort,\,max}(t)\big\}dt \end{aligned} \tag{6.2}$$

In a similar manner the energy index I_e [kWh] is defined, as shown in Equation 6.3 [15].

$$I_e = \int_{t=0}^{1\ year} P_{heating\ system}(t)dt \tag{6.3}$$

where $P_{heating\ system}$ is the power of the entire heating system (compressor, circulation pump, and heat pump fan).

The discomfort index is used to define the next performance indicator, namely discomfort days. A discomfort day is a day in which discomfort occurred, it only contains one discomfort type (undercooling/overheating). If on a single day both types occur, two discomfort days are counted.

6.3 Influence of Window Orientation

The controller is simulated in four similar dwellings, where the only difference is the orientation of the window. First, the thermal comfort is analysed; Figure 6.1 shows the performance differences between the orientations. Second, the energy index shows that the orientation of windows has a large effect on final energy consumption. The figure shows quite large relative differences between the scenarios. The difference of the energy index is explained with the fact that the window orientation plays an important role in heat gain by solar radiation. In Table 6.3 the energy demand per floor area is given, which is compared to the expected energy demand of an EPC-0.4 building in the Netherlands, which can be found in Table 5.3; for the sake of clarity it is repeated in Table 6.3. The efficiencies of the used heat pump system, and gas heater (reference building) are used to calculate the actual heat load of the building. Note that, as discussed earlier, that the amount of window surface per floor area is 2.8 times higher than in the simulated buildings; therefore, the results cannot be compared one to one. However, given the results in Table 6.3 the energy performance of the proposed controller is promising.

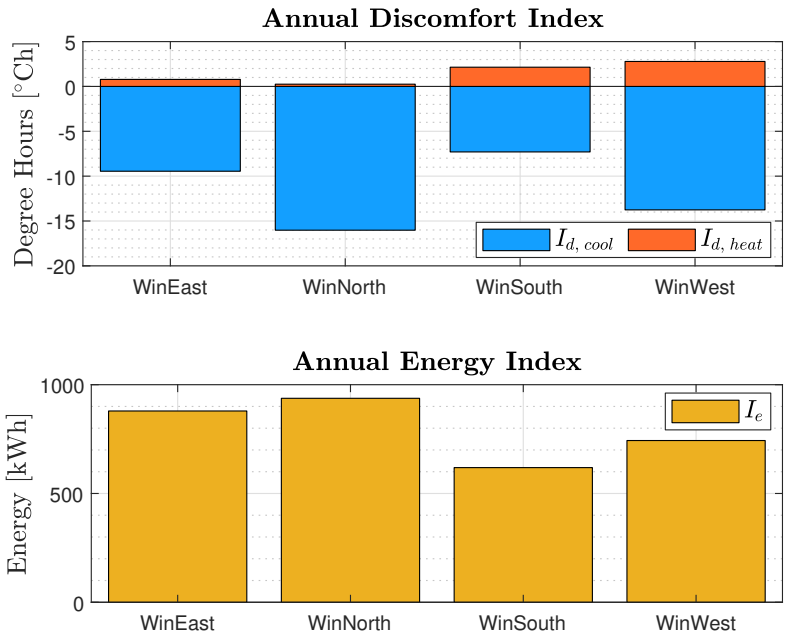

Figure 6.1: Annual discomfort and energy index comparison for four different window orientations.

Table 6.3: Total energy demand, corrected for heating system efficiencies.

Scenario	**Energy demand**
EPC-0.4 building	176 [MJ/m^2]
Window orientation: South	107 [MJ/m^2]
Window orientation: West	125 [MJ/m^2]
Window orientation: North	164 [MJ/m^2]
Window orientation: East	156 [MJ/m^2]

In order to determine whether the controller is usable in real applications it is necessary to analyse the differences on a daily level. This is done in Figure 6.2, where the total daily discomfort for the entire year is shown. The figure shows that the thermal discomfort in all cases is low, or is non-existent; with a peak of 0.74°Ch on November 24 (west orientation). In an attempt to put these values in perspective, the discomfort index of a rule based controller used by Maasoumy et al. [15] was on average 0.25°Ch per day (the absolute values for heating and cooling discomfort were merged together in that study), and the heuristically chosen maximum allowed discomfort index was set to 0.5°Ch.

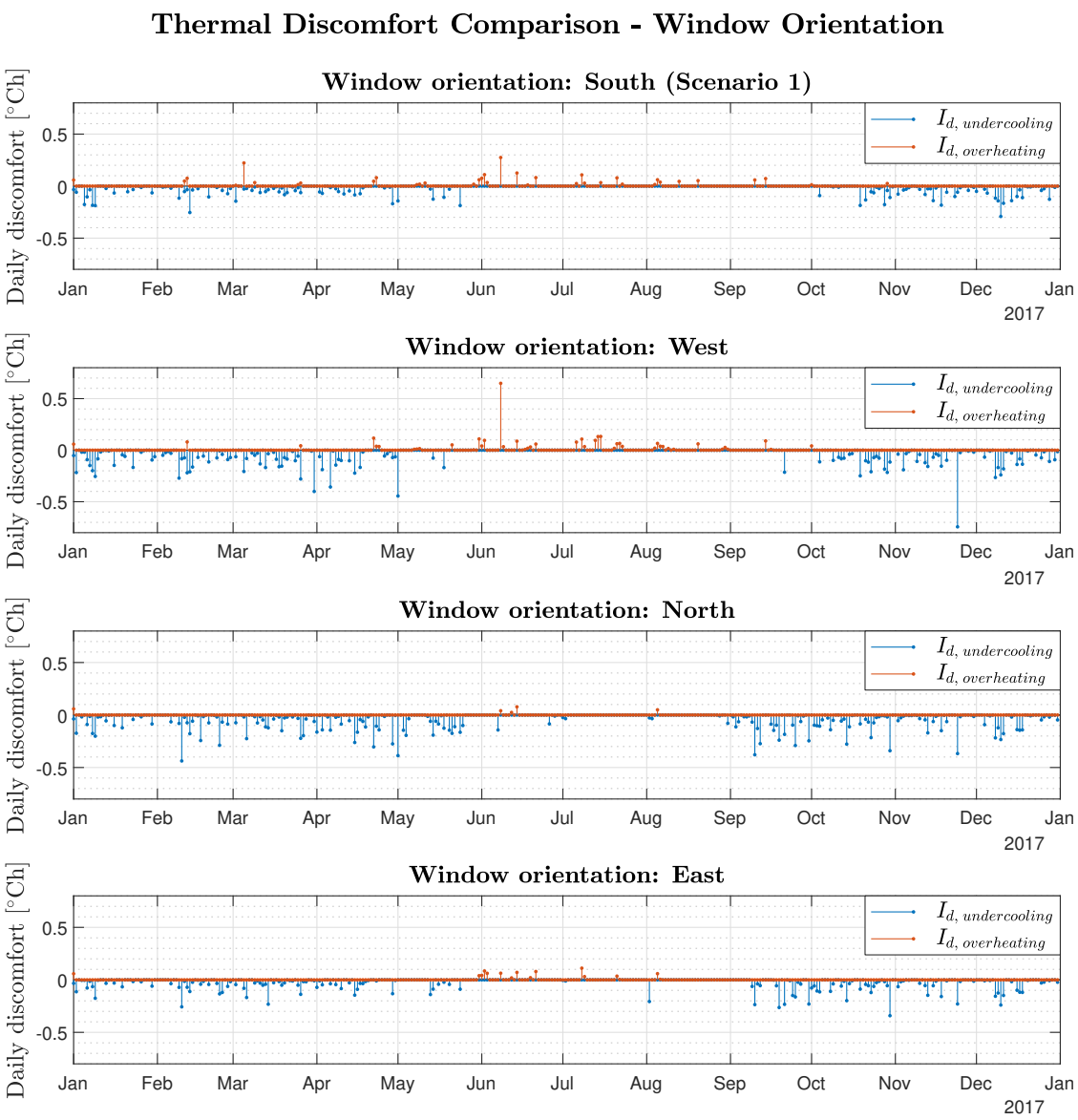

Figure 6.2: Overview of the daily discomfort during the year for four different window orientations.

Moreover, the controller shows consistent thermal behaviour for all orientations. This can also be seen in Figure 6.3, where the distribution of discomfort is shown. The figure shows that the amplitudes of the amount of discomfort is comparable, and lay mostly within the range [-0.3°Ch, 0.1°Ch].

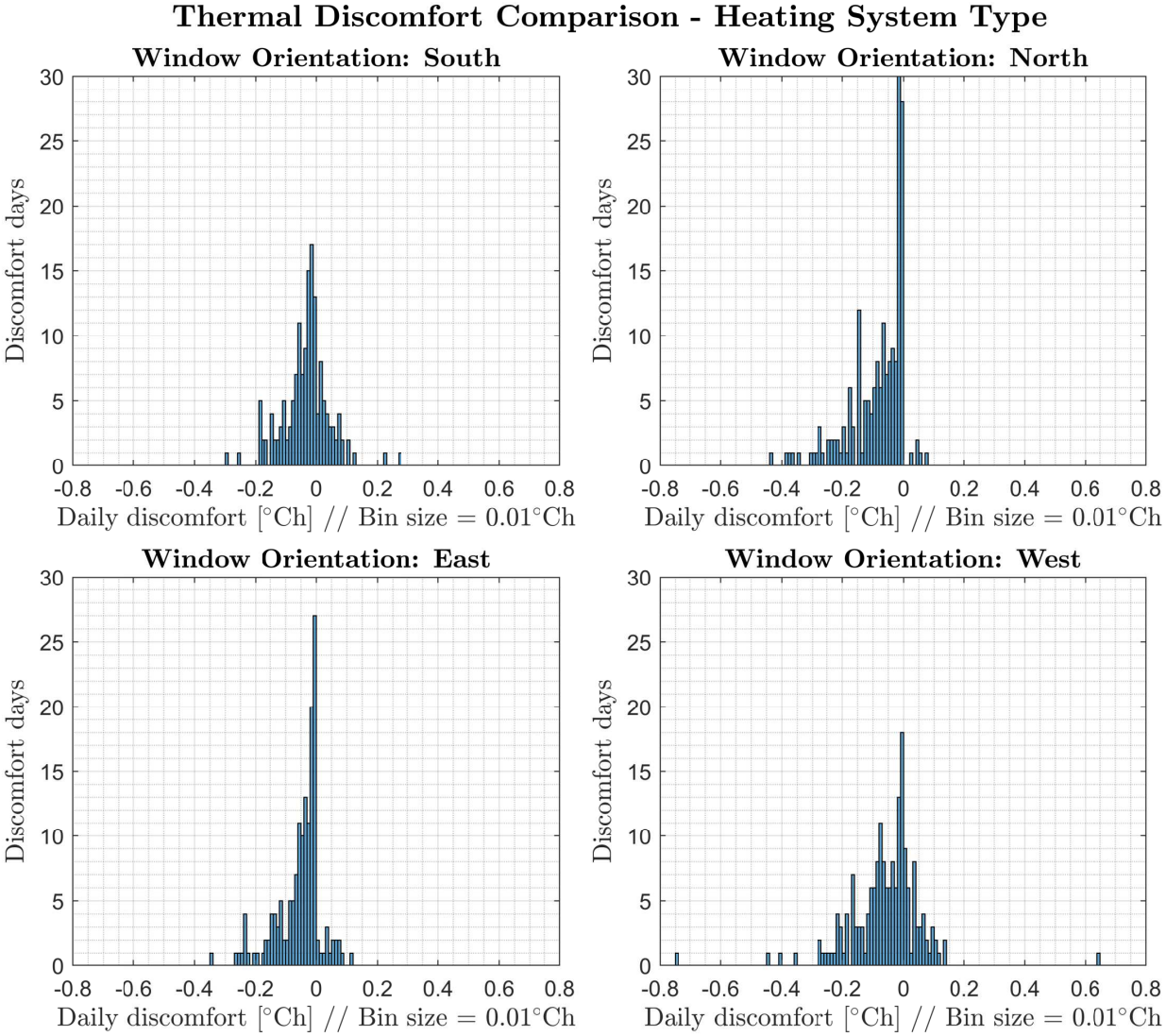

Figure 6.3: Distribution of the total discomfort days during a year, for all window orientations.

6.3.1 Undercooling Analysis

In order to understand what causes the peak on November 24, an analysis of that specific day is performed. Figure 6.4 shows the temperature profile of 24 hours, from the moment just before the controller decides to enable the heat pump. In addition, it shows the predicted optimal temperature profile, together with the optimal control actions based on estimated state information available at t=0 which represents 6:00h. The control actions of the shades, and the ventilation system are not shown, because the controller does not change the state (during the entire horizon, shades are opened, and ventilation is set to minimal). The observed state information is important to compute a proper forecast, because it is the starting point of the prediction, see Chapter 5.1. In the third sub-plot the temperature error of this estimated information is shown, which is defined in Equation 6.4. Although this value does not directly show the quality of the total state estimation, it gives an indication of the accuracy of the estimated temperature. Chapter 5.1 shows how the estimated temperature is calculated from the estimated states. Furthermore, the fourth sub-plot shows the simulated error based on actual model inputs, and is defined in Equation 6.5.

$$\epsilon_{observer}(t) = T_{actual}(t) - T_{observed}(t) \tag{6.4}$$

$$\epsilon_{forecast}(t) = T_{actual}(t) - (T_{simulated}(t) + \epsilon_{observer}(0)) \tag{6.5}$$

where T_{actual} is the simulated temperature inside the Modelica house, $T_{observed}$ is the temperature estimated by the Kalman filter, and $T_{simulated}$ is the simulated temperature by the ARX-based model, based on used control actions, measured disturbances, and the estimated state at start.

The fourth sub-plot in Figure 6.4 shows that the internal forecast model is not able to achieve a consistent low temperature error in the prediction. Furthermore, the Kalman filter was not specifically optimised, as discussed in Chapter 5.4, which results in errors in the state estimation. The observed temperature error, derived from the estimated states, is showed in the third sub-plot. Both reasons lead to control actions which are not optimal; in the current case it caused thermal discomfort at some moments during the day. In addition, the fact that there was no fast response heating system available (e.g. a radiator), and that during discomfort the heating system was already at maximum power, the controller was not able to regain thermal comfort in the short term.

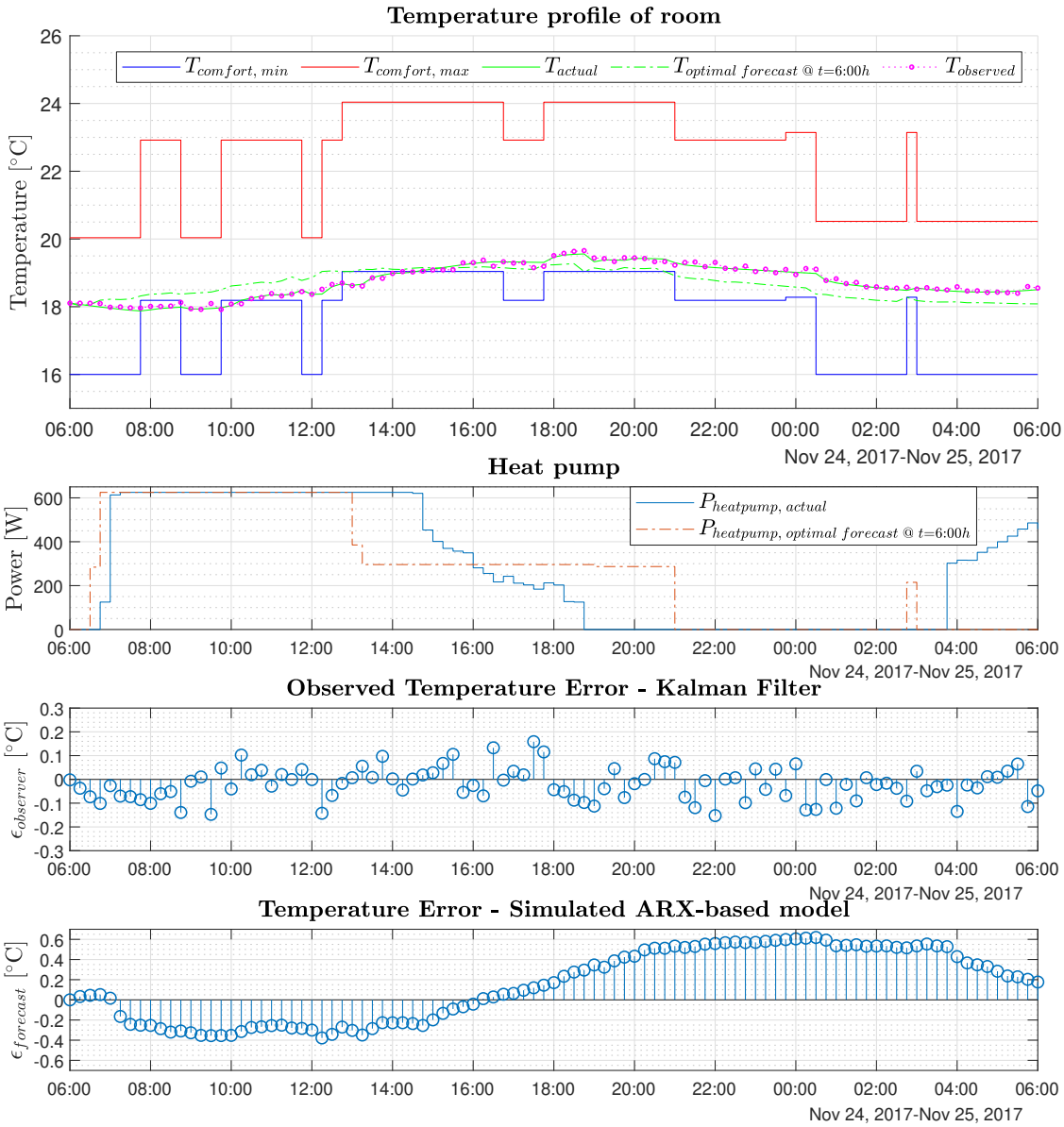

Figure 6.4: Thermal discomfort peak analysis of west oriented building on November 24.

Figure 6.5 shows the situation 24 hours earlier, where no thermal discomfort was registered. In this case the model shows comparable behaviour, however it tends to only underestimate the room temperature. It is expected that more energy than necessary is used, because generally the room temperature was well above the lower comfort bound. Another difference in this situation is the amount of heating power used; the controller is able to scale up power when necessary. This gives the system the ability to correct itself if there is a chance of thermal discomfort in the near future. Apart from the system's inability to predict the future temperature response more precise, it seems to be an exceptional combination of factors that caused the relatively large amount of discomfort on November 24.

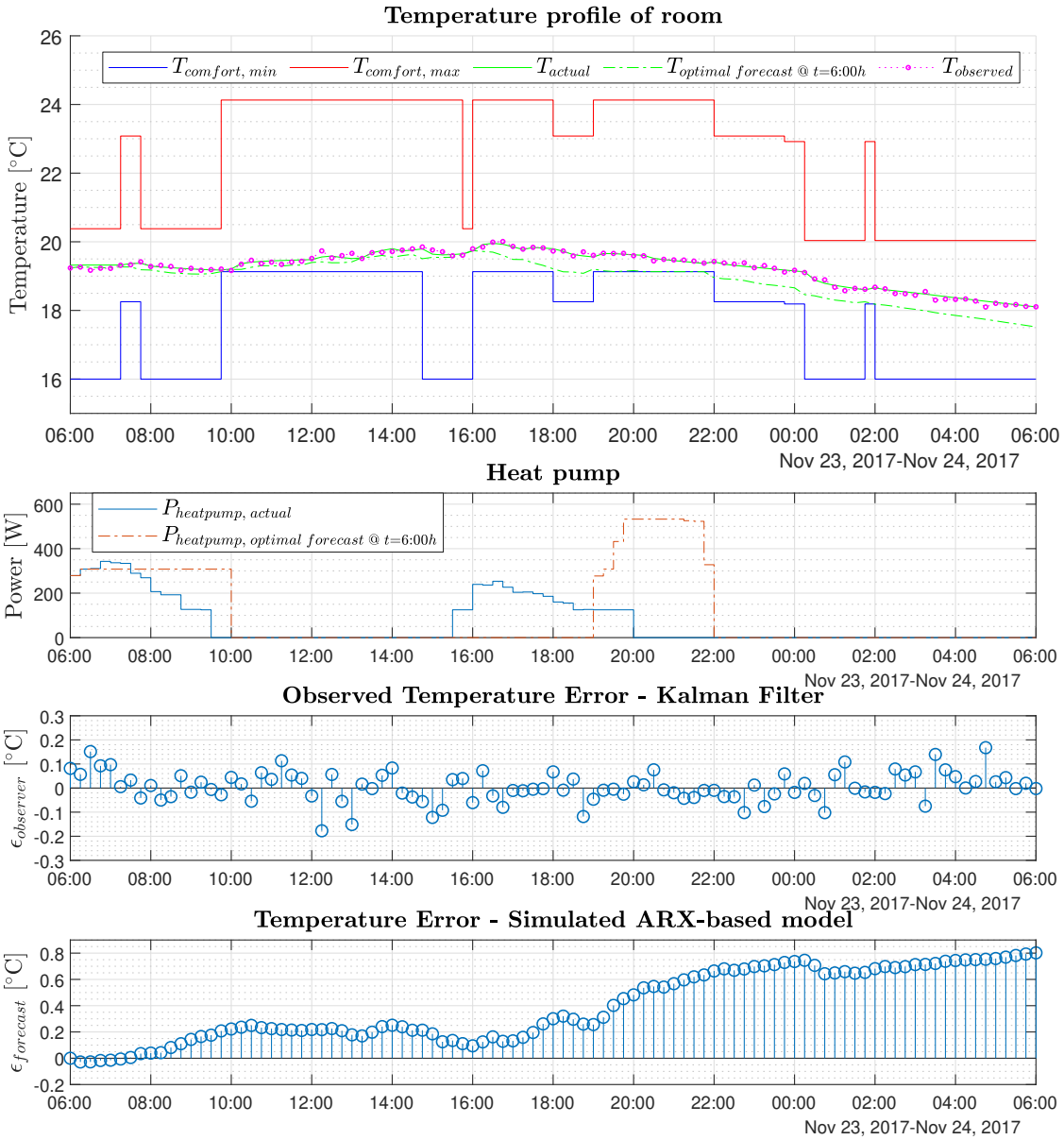

Figure 6.5: Profile of west oriented building on November 23.

6.3.2 Overheating Analysis

Figure 6.2 shows that on average overheating is hardly an issue; the biggest violation occurred on June 8 just after midnight, where relatively high thermal discomfort is registered. The profiles of this day are visualised in Figure 6.6. This figure shows the ventilation, and solar shading control actions; $P_{heat\ pump}$ is not shown, because it is not enabled during this period. In addition, the first sub-plot shows $T_{forecast,\,min.\,ventilation}$; which is the temperature forecast at t=0 (10:00h) where the ventilation is manually set to minimal. The solar shades are controlled as expected, by blocking a maximum amount of solar radiation. Taking into account the high insulation grade of the building, and the low occupancy rate of one person at that time, it is assumed that maximal ventilation should be the main cause of a rising temperature. However, the temperature profile for minimal and maximal ventilation is almost equal, while the ventilation heat flux is relatively high due to a higher outdoor temperature. As defined in Chapter 5.3.1.1 the optimisation problem

penalises the amount of discomfort. The maximum ventilation settings is, according to the forecast, a little bit in favour for the optimisation problem, because the difference between the upper comfort bound and the forecast is smaller than with the minimum ventilation setting. As a result, the ventilation was fully open, while minimal ventilation during the day probably would have given a better result, due to the high outdoor temperature. Moreover, the prediction accuracy is worse than the other analysed days; both effects indicate wrong understanding of ventilation effects within the prediction model, when outdoor temperatures are high. This might be a result of errors in model parameters obtained by the system identification procedure.

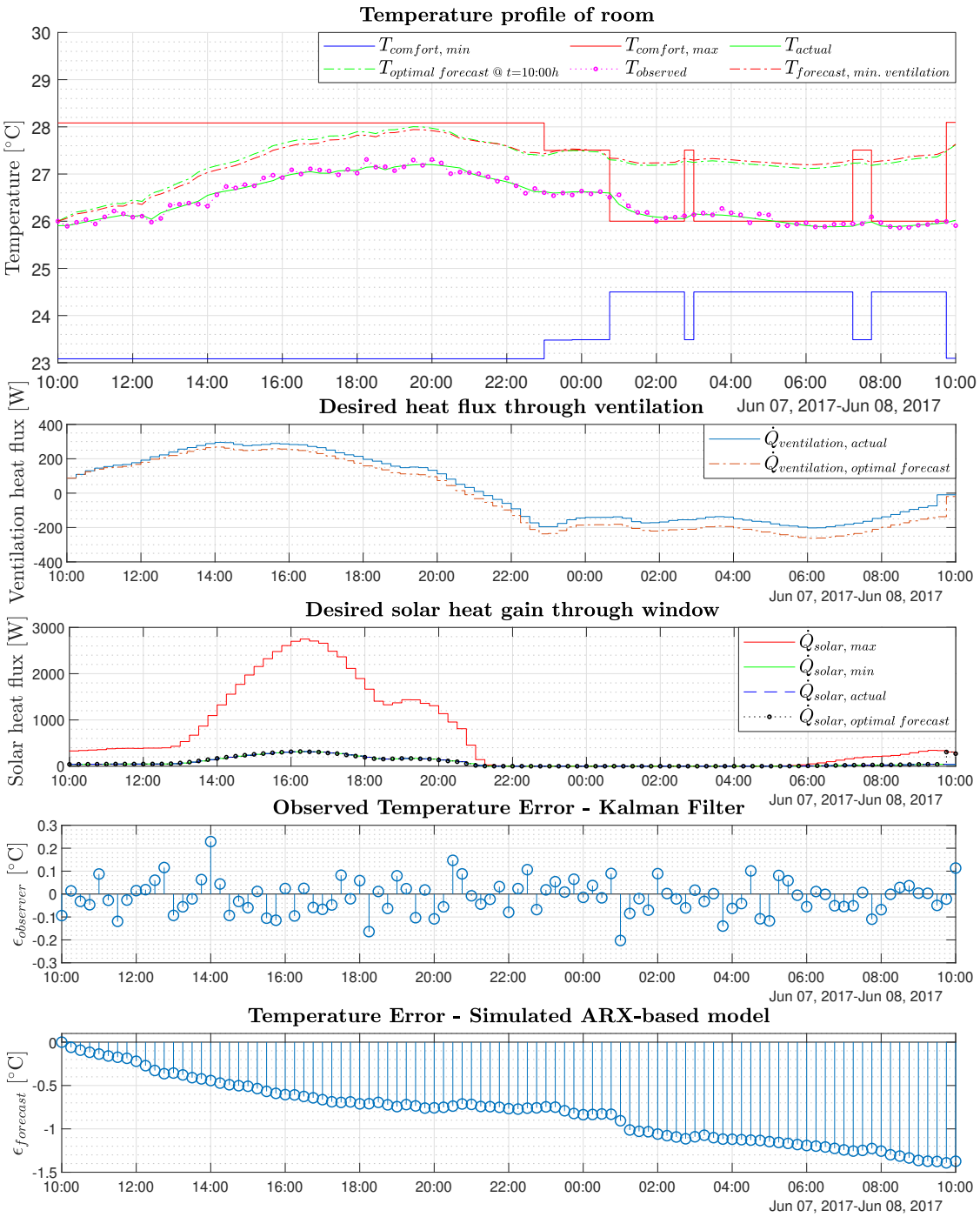

Figure 6.6: Profile of west oriented building on June 7-8.

6.4 Radiator-based Heating System

The next section discusses the analysis of the scenario with the radiator-based heating system. In this scenario, the floor heating system is replaced by a radiator, as discussed in Chapter 5.2. It is expected that the radiator can quickly respond to unforeseen thermal discomfort, due to the fast-response heating property of this type of system, compared with floor heating systems. The analysis is similar to the previous one, which implies that another peak analysis is performed, on

a thermal discomfort peak day.

6.4.1 Undercooling Analysis

Figure 6.7 shows the total annual difference between the two system types. The amount of undercooling discomfort is about 3 times larger for the radiator system, but with a significantly reduced energy consumption. To analyse the severity of the discomfort, a daily discomfort comparison is made, which is shown in Figure 6.8. Although the radiator system suffers from more thermal discomfort than the floor heating system, the amplitude of the daily discomfort is comparable, this is better visualised in Figure 6.9.

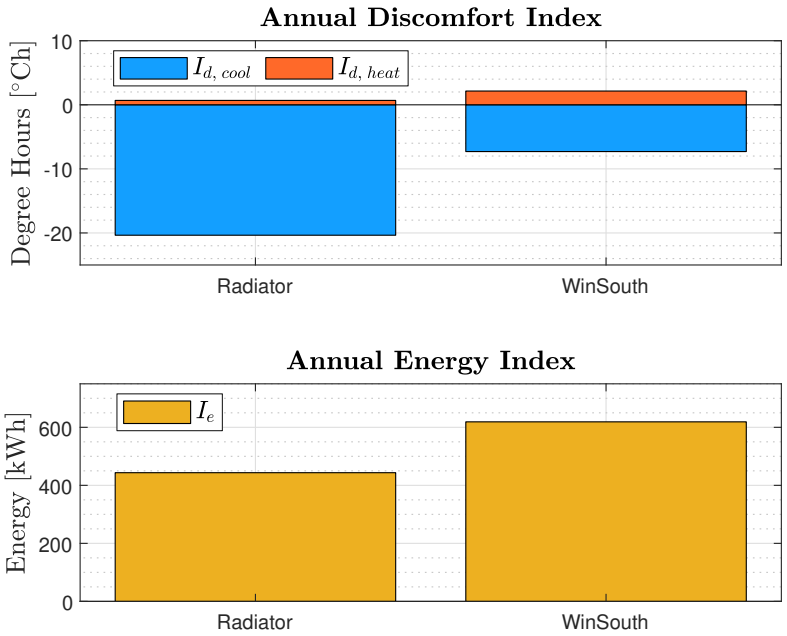

Figure 6.7: Annual discomfort and energy index comparison for floor- and radiator heating systems.

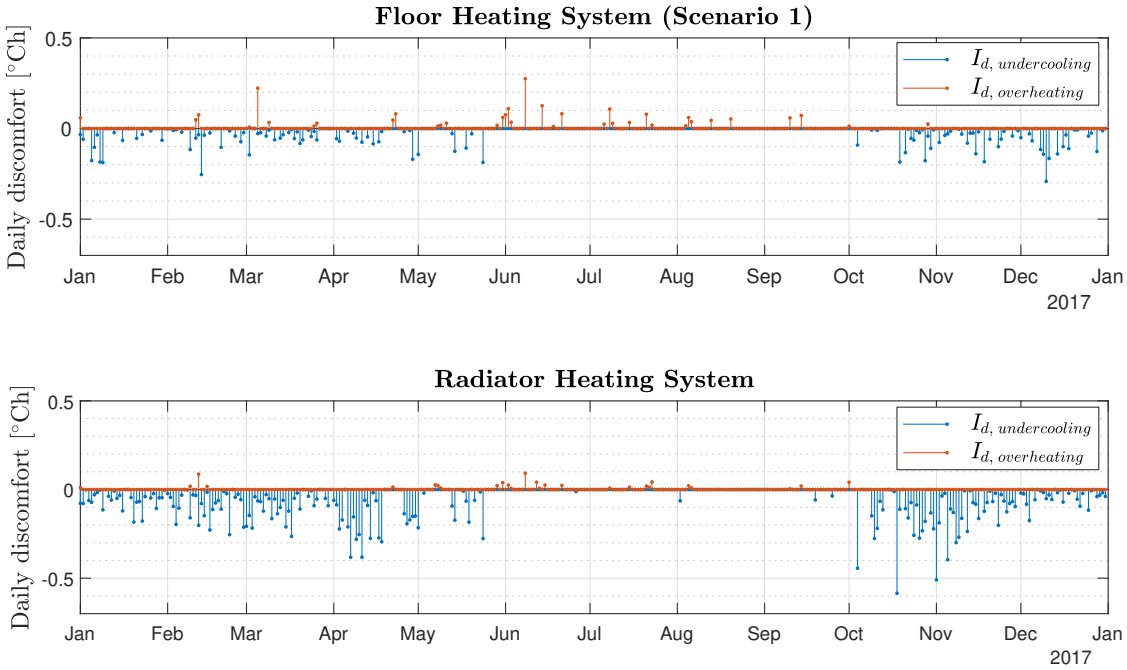

Figure 6.8: Overview of the daily discomfort during the year for floor- and radiator heating systems.

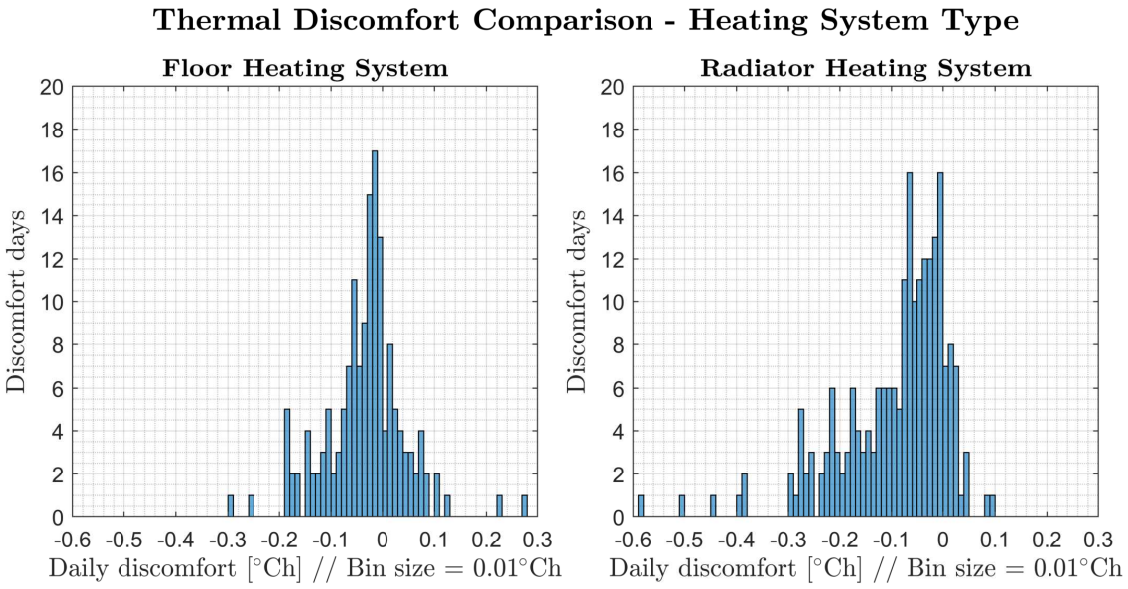

Figure 6.9: Distribution of the total discomfort days during a year, for both heating systems.

To complement Figure 6.3 & 6.9, the total amount of comfort/discomfort days for the five scenarios are given in Table 6.4. Note that the days do not count up to 365, due to the definition of a discomfort day, see Chapter 6.2.

Table 6.4: Total amount of discomfort days, and days without discomfort for five scenarios.

Scenario	**Discomfort days**	**Total days without discomfort**
Window Orientation: South	156	220
Window Orientation: North	187	179
Window Orientation: East	161	205
Window Orientation: West	186	182
Radiator Heating System	216	153

Figure 6.10 shows the temperature profile of the house, together with the control actions on October 18, just before the first thermal comfort violation occurred. October 18 is chosen because of the peak in thermal discomfort. The third and fourth sub-plots show the observed temperature error and the simulated temperature error, respectively. As expected, the radiator system is capable of quickly responding to thermal discomfort. However, the ARX-based model does not predict the optimal control actions well. The simulated temperature error shows that the model overestimates the actual temperature almost the entire horizon with values up to 1.2°C. This overestimation is significantly higher than the overestimation of the floor heating models. Moreover, the fast response property of the system, is modelled in the ARX-based model. Therefore, the observed temperature plays a more pronounced role, because there is less time to correct wrong behaviour based on wrong temperature estimations. As a result, the heat pump is sometimes started when there is already discomfort.

In addition, the controller shows notable behaviour around 3:30, which was caused by a large underestimation (up to 1.2°C) of the room temperature, based on observed states at 3:30. In order to avoid discomfort at 7:30 it computed an optimally economic trajectory which set the heat pump at a higher heating level. After the sudden increase in temperature the prediction performance improved again.

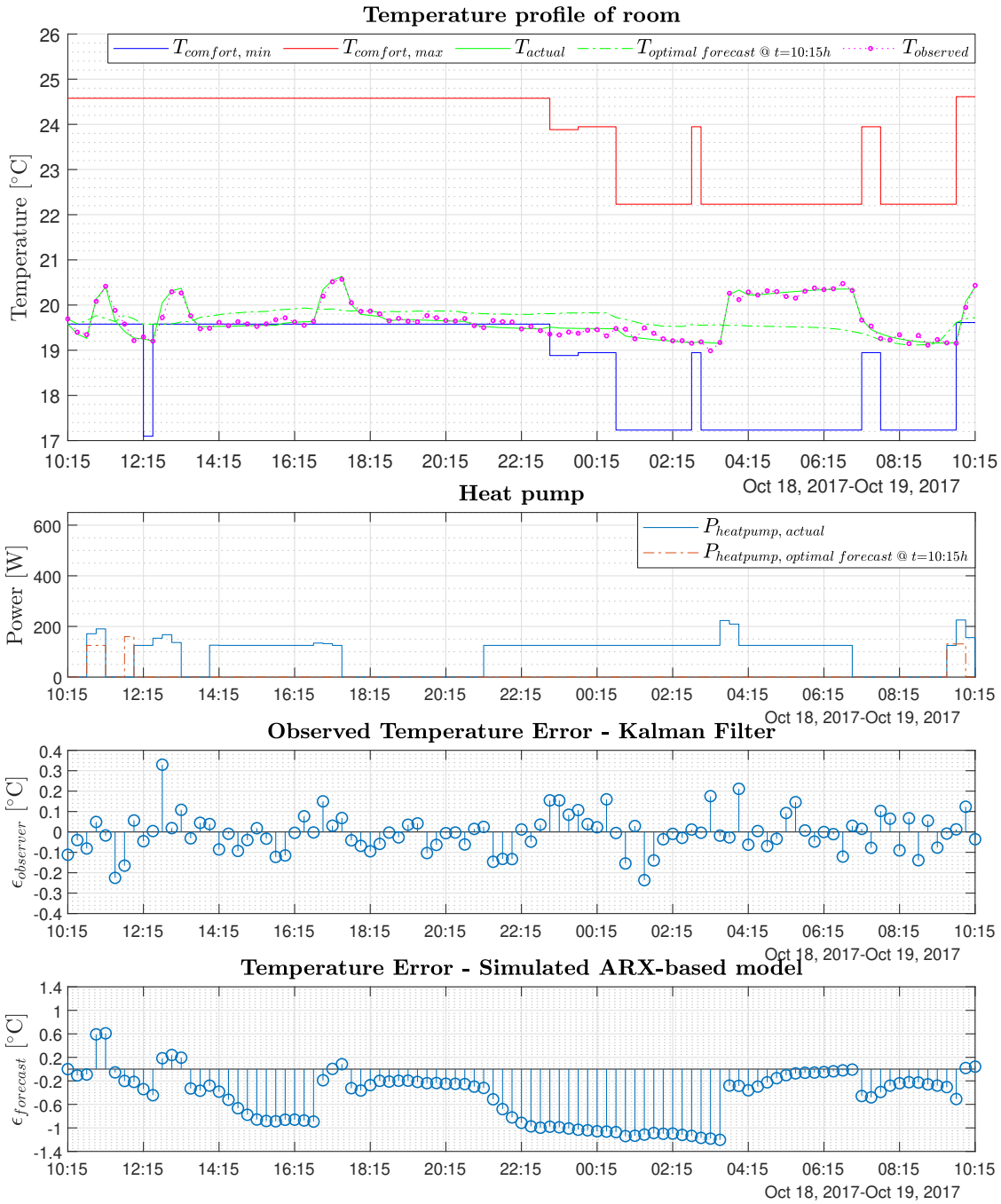

Figure 6.10: Thermal discomfort peak analysis of radiator heating system equipped building on October 18.

Figure 6.11 shows the situation 24 hours earlier, like in the previous paragraph, no thermal discomfort was registered. However, this is not due to proper estimation of the future control actions. The fourth sub-plot shows the error of the simulated temperature profile, the forecast tends to be more accurate when the heat pump is disabled. This behaviour is also visible in Figure 6.10, only it sometimes also shows a sudden increase in prediction performance when the heat pump state is changed. The model overestimates the temperature, which explains the bad optimal forecast of $P_{heat\ pump}$ in the second sub-plot. The Kalman filter shows comparable behaviour, but did not overestimate the indoor temperature, while it was near or below the lower thermal comfort bound.

An important factor between these days is the significant difference in occupancy behaviour, and as a result in thermal comfort bounds. Around 12:15 the minimal temperature drops for 15 minutes, and perhaps caused a decision of which the effect was underestimated by the forecast model. It can be concluded that the overestimation on both days, and the low prediction fit given in Table 6.2 is a strong indicator that the currently implemented ARX identification method is not suitable for houses with only a radiator system. Therefore, Chapter 6.5 discusses the analysis of the overall prediction accuracy for both systems.

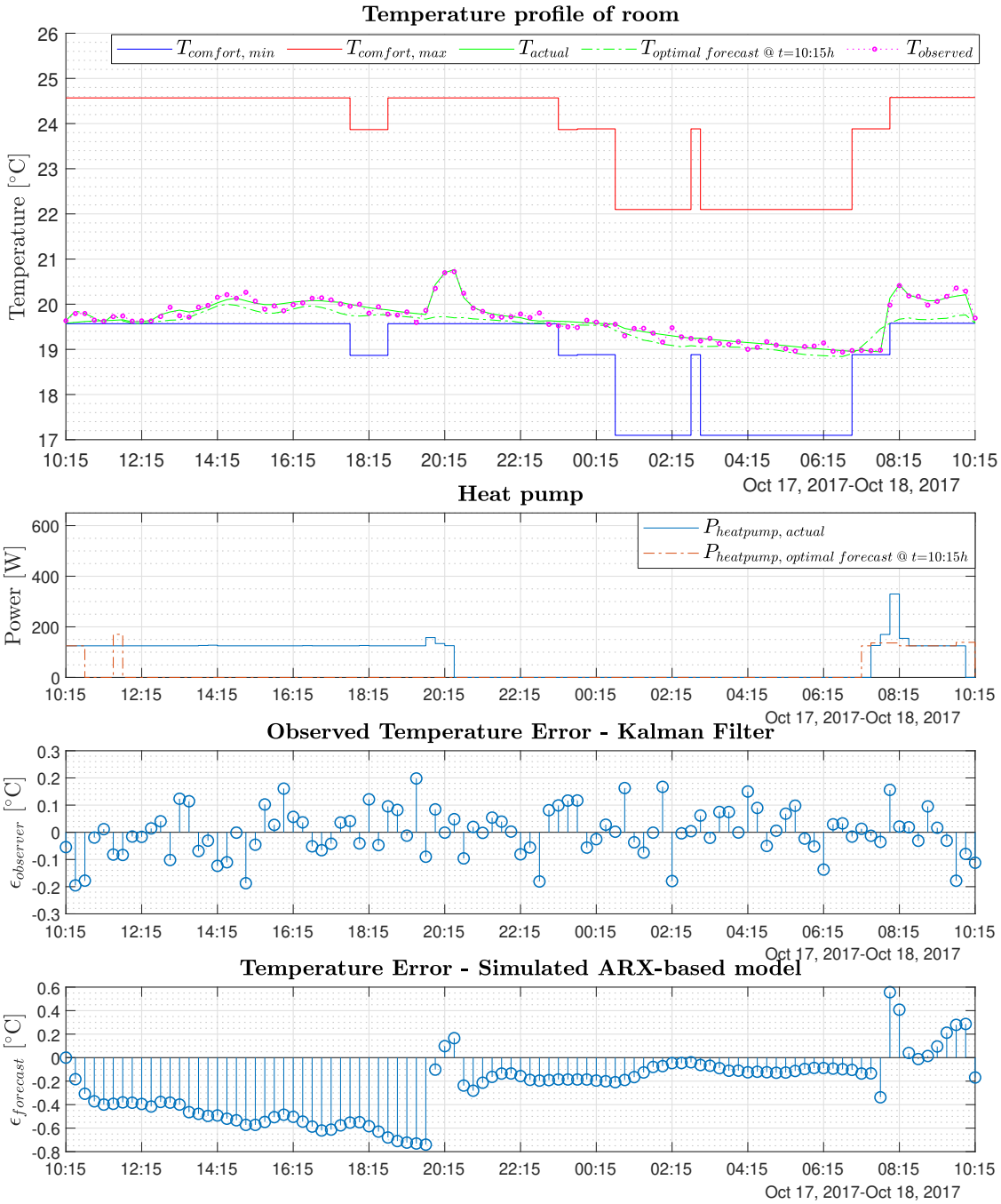

Figure 6.11: Profile of radiator heating system equipped building on October 17.

6.4.2 Overheating Analysis

Figure 6.8 shows that overheating is hardly an issue; the biggest violation occurred on June 8, where a small overheating peak is visible. The profiles of this day are visualised in Figure 6.12. The prediction performance shows a better result than in the undercooling case. It seems that the model has less difficulties predicting the temperature evolution when no additional heat is added via the heating system. This is also visible in Figure 6.10 & 6.11 of the undercooling analysis. Possibly, the variation in the heat pump power signal was not high enough during the system identification. Adaptive MPC approaches are possible solutions, because the controller then depends less on initial identification, but performs an online identification.

Moreover, when not in cooling mode, the current controller tries to maximise the amount of free heat gain, while staying within the thermal comfort bounds. As a consequence, it opens the solar shades in order to heat up the building, however cooling down without active cooling devices is slow. In this case the controller overestimated the temperature drop due to closing shades, and opening air-vents, which caused the minor thermal comfort violation.

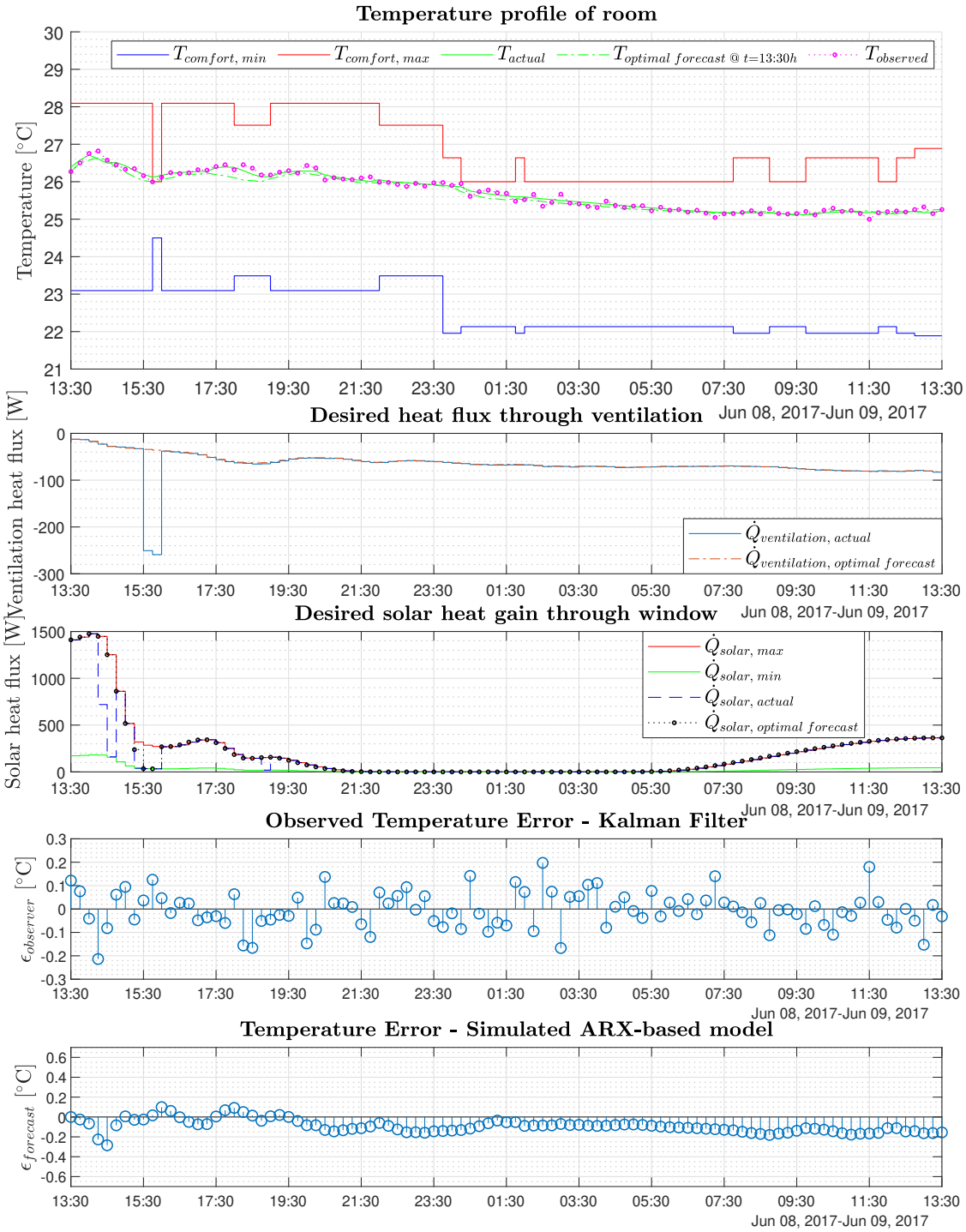

Figure 6.12: Profile of radiator heating system equipped building on June 8.

6.5 Forecast Analysis

Figure 6.13 shows the distribution of the forecast errors for every horizon step. The first-quartile contains 25% of the data set with the largest negative error, the interquartile-range contains the middle 50% and is split in half by the median, and the third-quartile contains 25% of the data

set with the largest positive error. On average the plot of the floor heating system shows that the predicted temperature is often lower than the actual temperature (a positive error). The model with the radiator heating system shows opposite behaviour. Moreover, the area of the interquartile-range is significantly narrower than the one with a radiator heating system, which implies that the forecast error is quite consistent. Furthermore, the outer quartiles are narrower which further results in a more consistent behaviour of the controller. These reasons explain the relatively low thermal discomfort occurrences in the floor heating scenario, compared to the radiator heating system. In addition, it explains the difference in energy use; due to the underestimation, the heat pump is used more often to heat the house in the case of the floor heating system.

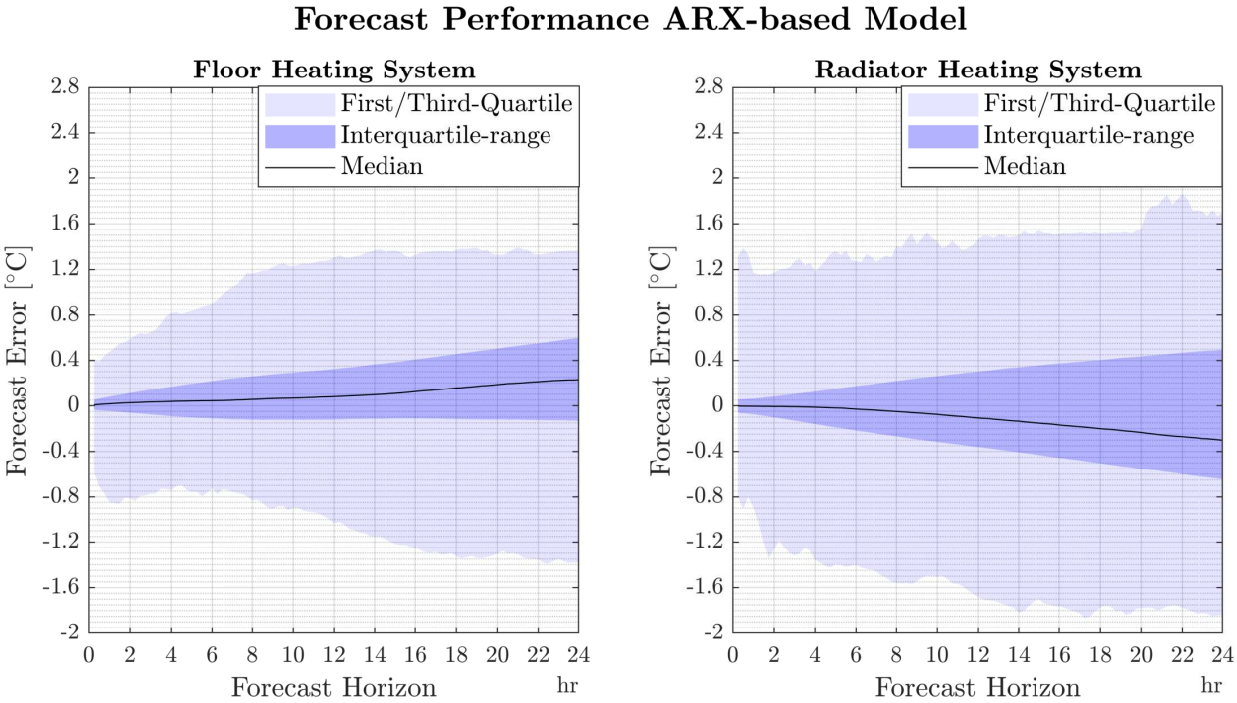

Figure 6.13: Forecast Performance of the internal ARX-based model of the MPC.

6.6 Disturbance Uncertainty Analysis

In order to analyse the influence of disturbance uncertainty, the resolution of disturbance preview is modified. In the default controller future disturbances are given up to 24 hours (the used horizon in this thesis) with a resolution of 15 minutes. For this analysis resolutions of 1, 3, and 6 hours are used, and the results are compared with the default resolution. A courser resolution is computed by averaging the disturbances over the resolution window; the disturbance at t=0 of the forecast is not modified. The floor heating system is implemented in this analysis. The following variables have a changed resolution:

- T_{out}
- H_{solar}
- $\dot{Q}_{occupancy}$
- $\dot{Q}_{solar,\,max}$
- $\dot{Q}_{solar,\,min}$

The last two variables are used as a constraint for the optimisation problem, in order to calculate $\dot{Q}_{solar}$ for the solar shading device, see Chapter 5.3. Figure 6.14 shows the annual discomfort, and energy index of the different scenarios. The disturbance resolution does not have a big influence

on the performance indices.

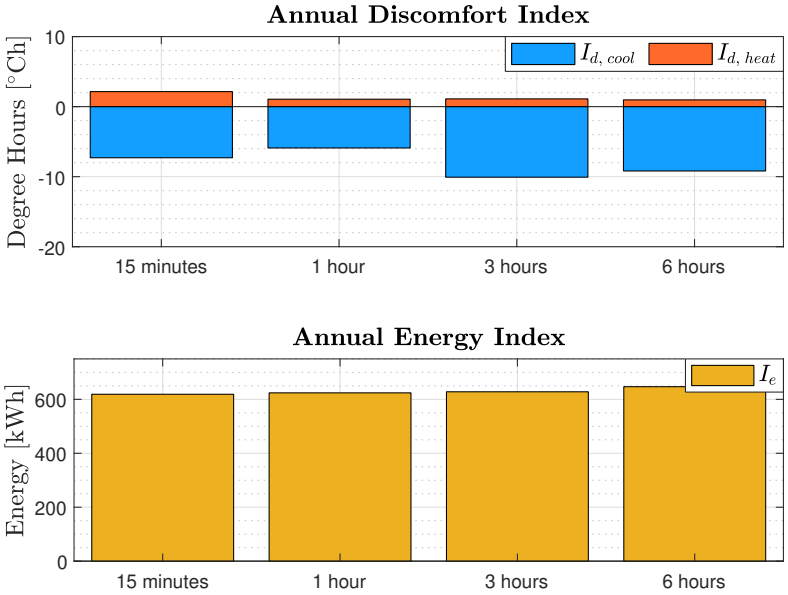

Figure 6.14: Annual discomfort and energy index comparison for four different disturbance resolutions.

Figure 6.15 shows the thermal discomfort distribution for each used resolution. Table 6.5 shows the total amount of discomfort days, combined with the total amount of days without discomfort. The behaviour of the controller is comparable regardless of the resolution. Possible explanations for this phenomenon are the high insulation, and thermal mass of the building, combined with the highly controllable solar heat gain through the window. In addition, solar heat gain is a fast-response action; therefore the current value, which is not affected by disturbance resolution, is more important than the forecast (future predicted control actions are discarded by the receding horizon control).

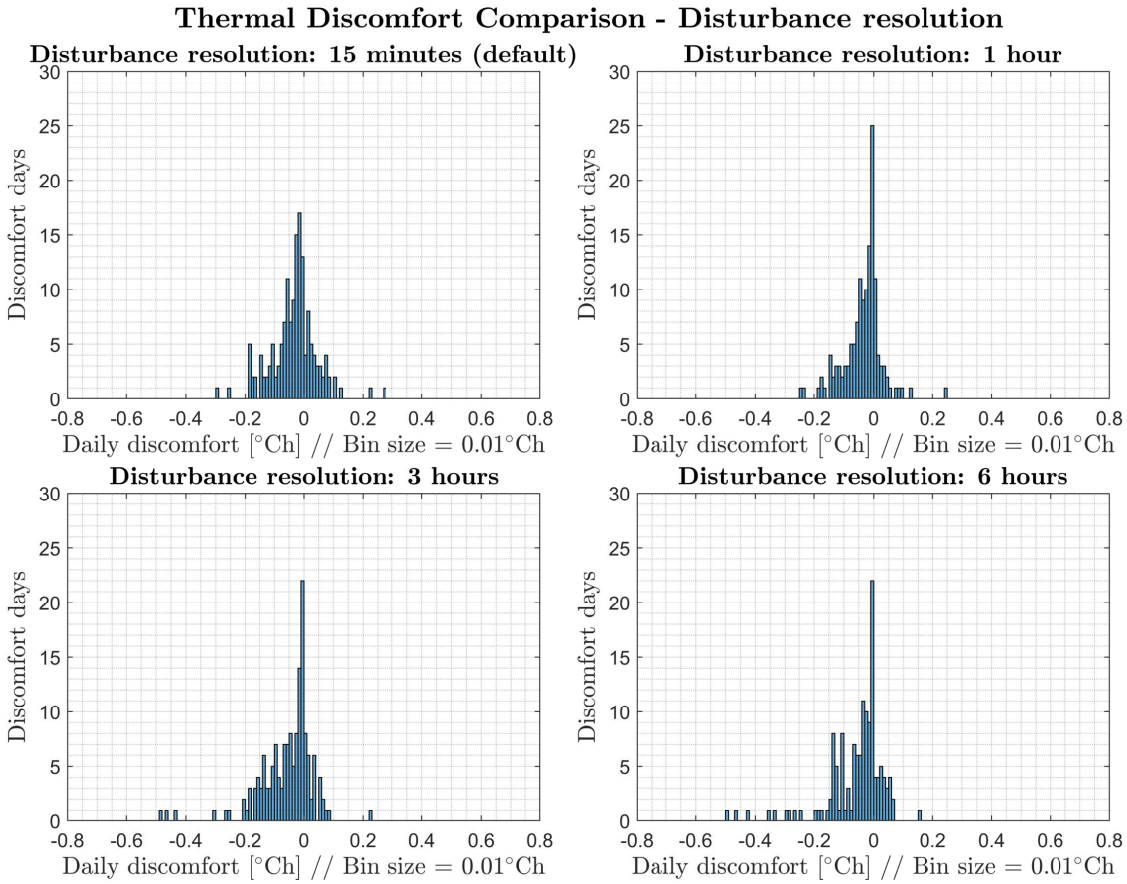

Figure 6.15: Distribution of the total discomfort days during a year, for both heating systems.

Table 6.5: Total amount of discomfort days, and days without discomfort for several disturbance resolutions.

Scenario	Discomfort days	Total days without discomfort
Disturbance resolution: 15 minutes	156	220
Disturbance resolution: 1 hour	141	234
Disturbance resolution: 3 hours	155	219
Disturbance resolution: 6 hours	140	233

6.7 Safety Margin on Comfort Bounds

In this section an analysis is performed on the impact of an offset on thermal comfort bounds. This offset is a type of safety margin to avoid thermal discomfort. The analysis is performed on both heating systems, and uses the same criteria as the previous analyses. First, in order to select a margin, the distribution of the observed temperature error of the Kalman filter is computed. The normal error distribution of both systems is shown in Figure 6.16, the mean and standard deviation are given in Table 6.6. The mean error is close to zero, and therefore can be neglected.

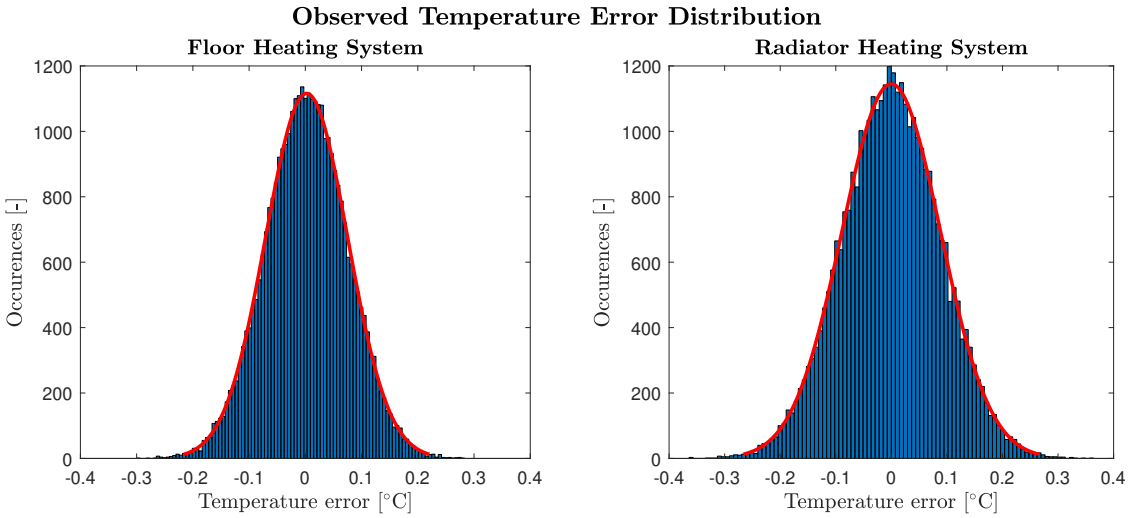

Figure 6.16: Distribution of the observed temperature error by the Kalman filter, for both heating systems. The red line is the fitted normal distribution.

Table 6.6: Normal distribution properties of Kalman estimation error.

Scenario	**Mean error (μ)**	**Standard deviation of error(σ)**
Floor Heating System	2.3e^{-3}°C	0.072°C
Radiator Heating System	-1.8e^{-4}°C	0.089°C

In a normal distribution 95% of the values are within interval [μ-2σ, μ+2σ]. For this reason an offset of 2σ is chosen as the size of the safety margin. This is done in the following analysis, in Figure 6.17 the annual performance indices of both systems are given, with and without the safety offset. It shows a significant reduction of thermal discomfort, however a slight increase (∼5%) in energy use is noticed.

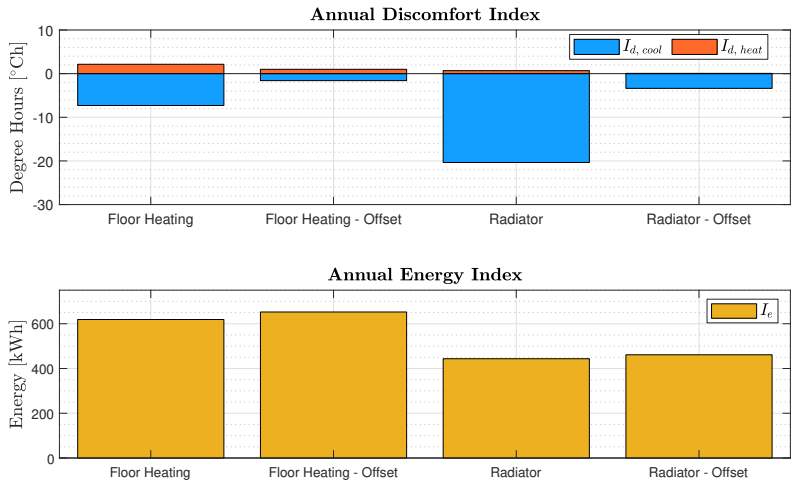

Figure 6.17: Annual discomfort and energy index comparison for four different disturbance resolutions.

Figure 6.18 and Table 6.7 show that the larger comfort violations are all eliminated, and the amount of days without discomfort is dramatically increased. Implementing the safety offset is a way to compensate for thermal discomfort caused by modelling imperfections, at the cost of a

slight increase of energy usage. Therefore, the priority should be on improving the internal forecast accuracy. This would potentially allow smaller safety margins to be used, reducing the energy cost.

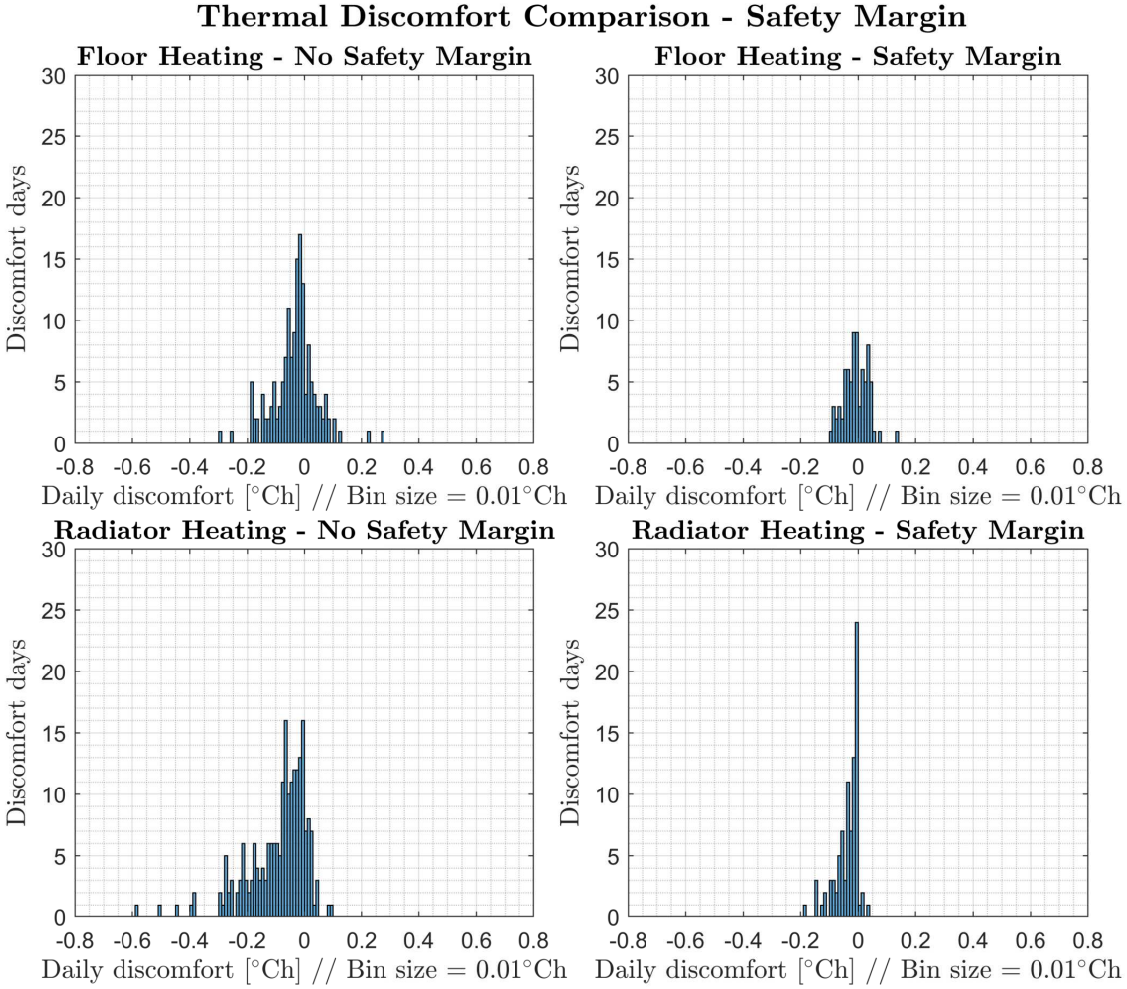

Figure 6.18: Distribution of the total discomfort days during a year, for both heating systems with and without safety margins on the thermal comfort constraints.

Table 6.7: Total amount of discomfort days, and days without discomfort for both heating systems with and without safety margins on the thermal comfort constraints.

Scenario	**Discomfort days**	**Total days without discomfort**
Floor Heating - Without Safety Offset	156	220
Floor Heating - With Safety Offset	76	293
Radiator Heating - Without Safety Offset	216	153
Radiator Heating - With Safety Offset	89	276

Conclusion

In this study a centralised data-driven HVAC controller was developed, in order to optimise energy usage while maintaining a thermally comfortable environment. Based on an extensive literature study, the data-driven method is chosen to be an ARX model, which was identified with a least square optimisation algorithm on data of a virtual target house. The initially obtained model prediction performance showed acceptable results, for implementation in a Model Predictive Control application. The identified model was used to perform a forecast over the next 24 hours, which was used to computed optimal control actions. It is important to note that the parameters for the Kalman filter were not optimised in this work, this leads to observed states which are less accurate. Consequently, only sub-optimal results can be achieved with the observed states. Therefore, the Kalman filter should be optimised to achieve better state estimation.

The first step of this analysis investigated the influence of window orientation on the controller's behaviour and performance. The analysis showed that the controller is able to handle different window orientations, with consistent behaviour. Given the notable differences in energy use for the different window orientations, and the comparable thermal discomfort behaviour, the controller is able to exploit energy of solar radiation, to keep the building within thermal comfort bounds by minimising electricity use.

The second step carried out an analysis regarding the radiator based heating system. The house with this type of system, showed better energy performance than the one with a floor heating system. However, there is no efficiency assessment performed for the different system types. Therefore, based solely on the results in this thesis, there can be no proper conclusion drawn regarding the difference in energy performance of the controller. Apart from that, based on the present analysis it can be assumed that the type of heating system (fast/slow-response) plays a significant role in the prediction performance. The forecast analysis showed that the prediction of the ARX model was more accurate in the case of the floor heating system. This could be due to the identification process, or it could be intrinsic to the modelling method. More research is required to draw any conclusion regarding this observation. As a result, the thermal comfort performance of this controller was better than the radiator heating system.

What is more, understanding of ventilation effects during high outdoor temperatures is not sufficient in the currently used ARX models, this may be due to an identification error. Misunderstanding of those effects could sometimes lead to overheating phenomena. However, in this work the overheating occurrences are low. The prediction performance of ventilation effects should be investigated further in future research.

The effects of forecast inaccuracies can be reduced by implementing a safety margin on the thermal comfort bounds. The margin chosen in this study, showed a large reduction in thermal discomfort, for a relatively small price in energy demand increase. However, improving the predictive capabilities of the model should be prioritised, in order to achieve optimal energy demand results.

The thermal discomfort which was observed in this study generally fits within the interval [-0.3°Ch, 0.1°Ch]. Previous research by Maasoumy et al. [15] used a maximum allowed discomfort index of 0.5°Ch. Reflecting this value on the present results, it can be concluded that the controller is able to maintain a thermally comfortable environment. Moreover, the MPC maintains thermal comfort even during summer, without active cooling devices. Furthermore, the energy demand shows promising results compared to expected energy use of an EPC-0.4 building. It is likely that energy and comfort performance increases when the internal prediction model, and the state observer are optimised.

Recommendations

Future research should focus on a better prediction accuracy of the internal model. This can possibly be achieved by using orthonormal basis filters, as shortly discussed in Chapter 5.1. These filters might also be useful for implementing adaptive MPC approaches [40]. An adaptive MPC method is believed to be the most viable option for commercial applications, due to the flexibility of the internal forecast model.

In addition, the current structure of the controller allows an improvement of thermal comfort prediction, when new insights in this field are available. It should also be noted that the current research assumed that future disturbances, e.g. occupant behaviour, were known (high or low resolution), which is not the case in real world scenarios. Further research is necessary to track and predict occupant behaviour, in order to improve temperature forecasts. Moreover, the controller does not take actual heat pump efficiency, and (future) electricity costs into account. Including these variables can further improve the economic benefits of the thermal comfort system.

Appendix A: Occupancy Profile

The used occupancy profile developed by Alders (2016) [6] is given in the following table, it is based on a household of two persons.

Time	Time	Living room	Kitchen	Master Bedroom	Bathroom
0	0	1	0	1	0
0.25	0.25	0	0	1	0
0.5	0.5	0	0	1	0
0.75	0.75	0	0	1	0
1	1	0	0	1	0
1.25	1.25	0	0	1	0
1.5	1.5	0	0	1	0
1.75	1.75	0	0	1	0
2	2	0	0	1	0
2.25	2.25	0	0	1	0
2.5	2.5	0	0	1	0
2.75	2.75	0	0	1	1
3	3	0	0	2	0
3.25	3.25	0	0	2	0
3.5	3.5	0	0	2	0
3.75	3.75	0	0	2	0
4	4	0	0	2	0
4.25	4.25	0	0	2	0
4.5	4.5	0	0	2	0
4.75	4.75	0	0	2	0
5	5	0	0	2	0
5.25	5.25	0	0	2	0
5.5	5.5	0	0	2	0
5.75	5.75	0	0	2	0
6	6	0	0	2	0
6.25	6.25	0	0	2	0
6.5	6.5	0	0	2	0
6.75	6.75	0	0	2	0
7	7	0	0	2	0
7.25	7.25	0	0	2	0
7.5	7.5	0	0	2	0
7.75	7.75	0	0	2	0
8	8	0	0	2	0
8.25	8.25	0	0	2	0
8.5	8.5	0	0	2	0
8.75	8.75	0	0	2	0
9	9	0	0	0	2
9.25	9.25	1	0	0	1
9.5	9.5	1	1	0	0
9.75	9.75	1	1	0	0
10	10	1	0	1	0
10.25	10.25	1	0	1	0
10.5	10.5	1	0	1	0
10.75	10.75	1	0	1	0
11	11	1	0	1	0

11.25	11.25	1	0	1	0
11.5	11.5	1	0	1	0
11.75	11.75	1	0	1	0
12	12	0	1	0	0
12.25	12.25	0	1	0	0
12.5	12.5	1	1	0	0
12.75	12.75	0	2	0	0
13	13	0	1	1	0
13.25	13.25	0	1	1	0
13.5	13.5	0	1	1	0
13.75	13.75	0	1	1	0
14	14	0	0	1	0
14.25	14.25	0	0	1	0
14.5	14.5	1	0	1	0
14.75	14.75	1	0	1	0
15	15	1	0	1	0
15.25	15.25	1	0	1	0
15.5	15.5	1	0	1	0
15.75	15.75	1	0	1	0
16	16	0	0	1	0
16.25	16.25	0	0	1	0
16.5	16.5	0	0	1	0
16.75	16.75	0	0	1	0
17	17	0	0	1	0
17.25	17.25	1	0	1	0
17.5	17.5	1	0	1	0
17.75	17.75	1	0	1	0
18	18	1	1	0	0
18.25	18.25	1	1	0	0
18.5	18.5	1	1	0	0
18.75	18.75	1	1	0	0
19	19	1	0	0	1
19.25	19.25	1	0	1	0
19.5	19.5	0	1	1	0
19.75	19.75	0	1	1	0
20	20	1	0	1	0
20.25	20.25	1	0	1	0
20.5	20.5	1	0	1	0
20.75	20.75	1	0	1	0
21	21	1	0	1	0
21.25	21.25	1	0	1	0
21.5	21.5	1	0	1	0
21.75	21.75	1	0	1	0
22	22	0	0	1	1
22.25	22.25	0	0	2	0
22.5	22.5	0	0	2	0
22.75	22.75	0	0	2	0
23	23	0	0	2	0
23.25	23.25	0	0	2	0
23.5	23.5	0	0	2	0
23.75	23.75	0	0	2	0

0	24	0	0	1	0
0.25	24.25	0	0	1	0
0.5	24.5	0	0	1	0
0.75	24.75	0	0	1	0
1	25	0	0	1	0
1.25	25.25	0	0	1	0
1.5	25.5	0	0	1	0
1.75	25.75	0	0	1	0
2	26	0	0	1	0
2.25	26.25	0	0	1	0
2.5	26.5	0	0	1	1
2.75	26.75	0	0	2	0
3	27	0	0	2	0
3.25	27.25	0	0	2	0
3.5	27.5	0	0	2	0
3.75	27.75	0	0	2	0
4	28	0	0	2	0
4.25	28.25	0	0	2	0
4.5	28.5	0	0	2	0
4.75	28.75	0	0	2	0
5	29	0	0	2	0
5.25	29.25	0	0	2	0
5.5	29.5	0	0	2	0
5.75	29.75	0	0	2	0
6	30	0	0	2	0
6.25	30.25	0	0	2	0
6.5	30.5	0	0	2	0
6.75	30.75	0	0	2	0
7	31	0	0	2	0
7.25	31.25	0	0	2	0
7.5	31.5	0	0	2	0
7.75	31.75	0	0	2	0
8	32	0	0	2	0
8.25	32.25	0	0	2	0
8.5	32.5	0	0	2	0
8.75	32.75	0	0	1	1
9	33	0	0	1	1
9.25	33.25	0	0	1	1
9.5	33.5	0	0	1	1
9.75	33.75	0	0	2	0
10	34	0	0	2	0
10.25	34.25	0	0	2	0
10.5	34.5	0	0	1	1
10.75	34.75	0	0	1	0
11	35	0	0	0	1
11.25	35.25	0	0	0	0
11.5	35.5	0	0	0	0
11.75	35.75	0	0	0	0
12	36	1	1	0	0
12.25	36.25	1	1	0	0
12.5	36.5	1	1	0	0

12.75	36.75	2	0	0	0
13	37	2	0	0	0
13.25	37.25	2	0	0	0
13.5	37.5	2	0	0	0
13.75	37.75	2	0	0	0
14	38	2	0	0	0
14.25	38.25	2	0	0	0
14.5	38.5	2	0	0	0
14.75	38.75	2	0	0	0
15	39	2	0	0	0
15.25	39.25	2	0	0	0
15.5	39.5	2	0	0	0
15.75	39.75	2	0	0	0
16	40	1	0	0	1
16.25	40.25	1	0	0	1
16.5	40.5	1	0	0	1
16.75	40.75	1	0	0	1
17	41	1	0	0	1
17.25	41.25	1	0	0	1
17.5	41.5	2	0	0	0
17.75	41.75	2	0	0	0
18	42	1	0	0	0
18.25	42.25	1	0	0	0
18.5	42.5	1	0	0	0
18.75	42.75	1	0	0	0
19	43	1	0	0	0
19.25	43.25	1	0	0	0
19.5	43.5	1	0	0	0
19.75	43.75	1	0	0	0
20	44	0	1	0	0
20.25	44.25	1	0	0	0
20.5	44.5	1	0	0	0
20.75	44.75	1	0	0	0
21	45	2	0	0	0
21.25	45.25	2	0	0	0
21.5	45.5	2	0	0	0
21.75	45.75	2	0	0	0
22	46	2	0	0	0
22.25	46.25	2	0	0	0
22.5	46.5	2	0	0	0
22.75	46.75	2	0	0	0
23	47	1	0	1	0
23.25	47.25	1	0	1	0
23.5	47.5	1	0	1	0
23.75	47.75	1	0	1	0
0	48	0	0	1	0
0.25	48.25	0	0	1	0
0.5	48.5	0	0	1	0
0.75	48.75	0	0	1	0
1	49	0	0	1	0
1.25	49.25	0	0	1	0

1.5	49.5	0	0	1	0
1.75	49.75	0	0	1	0
2	50	0	0	1	1
2.25	50.25	0	0	2	0
2.5	50.5	0	0	2	0
2.75	50.75	0	0	2	0
3	51	0	0	2	0
3.25	51.25	0	0	2	0
3.5	51.5	0	0	2	0
3.75	51.75	0	0	2	0
4	52	0	0	2	0
4.25	52.25	0	0	2	0
4.5	52.5	0	0	2	0
4.75	52.75	0	0	2	0
5	53	0	0	2	0
5.25	53.25	0	0	2	0
5.5	53.5	0	0	2	0
5.75	53.75	0	0	2	0
6	54	0	0	2	0
6.25	54.25	0	0	2	0
6.5	54.5	0	0	1	1
6.75	54.75	0	0	1	1
7	55	0	0	1	1
7.25	55.25	1	0	1	0
7.5	55.5	1	0	1	0
7.75	55.75	1	0	1	0
8	56	1	0	1	0
8.25	56.25	1	0	1	0
8.5	56.5	1	0	1	0
8.75	56.75	1	0	1	0
9	57	1	0	1	0
9.25	57.25	1	0	1	0
9.5	57.5	1	0	1	0
9.75	57.75	1	0	1	0
10	58	1	0	0	1
10.25	58.25	2	0	0	0
10.5	58.5	2	0	0	0
10.75	58.75	2	0	0	0
11	59	2	0	0	0
11.25	59.25	2	0	0	0
11.5	59.5	2	0	0	0
11.75	59.75	2	0	0	0
12	60	0	1	0	0
12.25	60.25	0	1	0	0
12.5	60.5	1	0	0	0
12.75	60.75	1	1	0	0
13	61	1	1	0	0
13.25	61.25	1	1	0	0
13.5	61.5	2	0	0	0
13.75	61.75	2	0	0	0
14	62	2	0	0	0

14.25	62.25	2	0	0	0
14.5	62.5	2	0	0	0
14.75	62.75	2	0	0	0
15	63	1	0	0	0
15.25	63.25	1	0	0	0
15.5	63.5	1	0	0	0
15.75	63.75	1	0	0	0
16	64	1	0	0	0
16.25	64.25	1	0	0	0
16.5	64.5	1	0	0	0
16.75	64.75	1	0	0	0
17	65	1	0	0	0
17.25	65.25	1	0	0	0
17.5	65.5	2	0	0	0
17.75	65.75	2	0	0	0
18	66	1	0	1	0
18.25	66.25	1	0	1	0
18.5	66.5	1	0	1	0
18.75	66.75	1	0	1	0
19	67	2	0	0	0
19.25	67.25	2	0	0	0
19.5	67.5	2	0	0	0
19.75	67.75	2	0	0	0
20	68	1	0	0	0
20.25	68.25	1	1	0	0
20.5	68.5	1	1	0	0
20.75	68.75	2	0	0	0
21	69	2	0	0	0
21.25	69.25	2	0	0	0
21.5	69.5	2	0	0	0
21.75	69.75	2	0	0	0
22	70	2	0	0	0
22.25	70.25	2	0	0	0
22.5	70.5	1	0	0	0
22.75	70.75	1	0	0	0
23	71	2	0	0	0
23.25	71.25	2	0	0	0
23.5	71.5	1	0	1	0
23.75	71.75	1	0	1	0
0	72	1	0	1	0
0.25	72.25	1	0	1	0
0.5	72.5	1	0	1	0
0.75	72.75	1	0	1	0
1	73	0	0	1	0
1.25	73.25	0	0	1	0
1.5	73.5	0	0	1	0
1.75	73.75	0	0	1	0
2	74	0	0	1	0
2.25	74.25	0	0	1	0
2.5	74.5	0	0	1	0
2.75	74.75	0	0	1	0

3	75	0	0	1	1
3.25	75.25	0	0	2	0
3.5	75.5	0	0	2	0
3.75	75.75	0	0	2	0
4	76	0	0	2	0
4.25	76.25	0	0	2	0
4.5	76.5	0	0	2	0
4.75	76.75	0	0	2	0
5	77	0	0	2	0
5.25	77.25	0	0	2	0
5.5	77.5	0	0	2	0
5.75	77.75	0	0	2	0
6	78	0	0	2	0
6.25	78.25	0	0	2	0
6.5	78.5	0	0	2	0
6.75	78.75	0	0	2	0
7	79	0	0	2	0
7.25	79.25	1	0	1	0
7.5	79.5	0	0	1	1
7.75	79.75	0	0	1	1
8	80	1	0	1	0
8.25	80.25	1	0	0	1
8.5	80.5	1	0	0	1
8.75	80.75	1	0	0	1
9	81	1	0	0	0
9.25	81.25	1	0	0	0
9.5	81.5	2	0	0	0
9.75	81.75	2	0	0	0
10	82	2	0	0	0
10.25	82.25	1	0	0	0
10.5	82.5	1	0	0	0
10.75	82.75	1	0	0	0
11	83	1	0	0	0
11.25	83.25	1	0	0	0
11.5	83.5	1	0	0	0
11.75	83.75	1	0	0	0
12	84	0	1	0	0
12.25	84.25	0	1	0	0
12.5	84.5	0	0	0	0
12.75	84.75	0	1	0	0
13	85	0	1	0	0
13.25	85.25	0	1	0	0
13.5	85.5	0	1	0	0
13.75	85.75	0	1	0	0
14	86	1	0	0	0
14.25	86.25	1	0	0	0
14.5	86.5	1	0	0	0
14.75	86.75	1	0	0	0
15	87	1	0	0	0
15.25	87.25	1	0	0	0
15.5	87.5	1	0	0	0

15.75	87.75	1	0	0	0
16	88	2	0	0	0
16.25	88.25	2	0	0	0
16.5	88.5	2	0	0	0
16.75	88.75	2	0	0	0
17	89	1	0	0	0
17.25	89.25	1	0	0	0
17.5	89.5	2	0	0	0
17.75	89.75	2	0	0	0
18	90	2	0	0	0
18.25	90.25	1	1	0	0
18.5	90.5	1	1	0	0
18.75	90.75	2	0	0	0
19	91	1	1	0	0
19.25	91.25	1	1	0	0
19.5	91.5	1	1	0	0
19.75	91.75	1	1	0	0
20	92	1	1	0	0
20.25	92.25	1	1	0	0
20.5	92.5	1	1	0	0
20.75	92.75	1	1	0	0
21	93	2	0	0	0
21.25	93.25	2	0	0	0
21.5	93.5	2	0	0	0
21.75	93.75	2	0	0	0
22	94	2	0	0	0
22.25	94.25	2	0	0	0
22.5	94.5	2	0	0	0
22.75	94.75	2	0	0	0
23	95	1	0	0	1
23.25	95.25	1	0	1	0
23.5	95.5	1	0	1	0
23.75	95.75	1	0	1	0
0	96	1	0	1	0
0.25	96.25	1	0	1	0
0.5	96.5	1	0	1	0
0.75	96.75	1	0	1	0
1	97	0	0	1	0
1.25	97.25	0	0	1	0
1.5	97.5	0	0	1	0
1.75	97.75	0	0	1	0
2	98	0	0	1	0
2.25	98.25	0	0	1	0
2.5	98.5	0	0	1	0
2.75	98.75	0	0	1	0
3	99	0	0	1	1
3.25	99.25	0	0	2	0
3.5	99.5	0	0	2	0
3.75	99.75	0	0	2	0
4	100	0	0	2	0
4.25	100.25	0	0	2	0

4.5	100.5	0	0	2	0
4.75	100.75	0	0	2	0
5	101	0	0	2	0
5.25	101.25	0	0	2	0
5.5	101.5	0	0	2	0
5.75	101.75	0	0	2	0
6	102	0	0	2	0
6.25	102.25	0	0	2	0
6.5	102.5	0	0	2	0
6.75	102.75	0	0	2	0
7	103	0	0	2	0
7.25	103.25	0	0	2	0
7.5	103.5	0	0	1	1
7.75	103.75	0	0	1	1
8	104	0	0	1	0
8.25	104.25	0	0	1	0
8.5	104.5	0	0	1	0
8.75	104.75	0	0	1	0
9	105	0	0	1	0
9.25	105.25	0	0	1	0
9.5	105.5	0	0	1	0
9.75	105.75	0	0	1	0
10	106	0	0	0	1
10.25	106.25	2	0	0	0
10.5	106.5	2	0	0	0
10.75	106.75	2	0	0	0
11	107	2	0	0	0
11.25	107.25	2	0	0	0
11.5	107.5	2	0	0	0
11.75	107.75	2	0	0	0
12	108	2	0	0	0
12.25	108.25	1	1	0	0
12.5	108.5	1	1	0	0
12.75	108.75	2	0	0	0
13	109	1	0	0	0
13.25	109.25	1	0	0	0
13.5	109.5	1	1	0	0
13.75	109.75	1	1	0	0
14	110	1	1	0	0
14.25	110.25	1	0	0	0
14.5	110.5	1	0	0	0
14.75	110.75	1	0	0	0
15	111	0	0	0	0
15.25	111.25	0	0	0	0
15.5	111.5	0	0	0	0
15.75	111.75	0	0	0	0
16	112	0	0	1	0
16.25	112.25	1	0	0	0
16.5	112.5	1	0	0	0
16.75	112.75	1	0	0	0
17	113	1	0	0	0

17.25	113.25	1	0	0	0
17.5	113.5	1	1	0	0
17.75	113.75	1	1	0	0
18	114	1	1	0	0
18.25	114.25	1	0	1	0
18.5	114.5	0	1	1	0
18.75	114.75	0	1	1	0
19	115	0	1	1	0
19.25	115.25	1	1	0	0
19.5	115.5	1	1	0	0
19.75	115.75	1	1	0	0
20	116	1	1	0	0
20.25	116.25	1	1	0	0
20.5	116.5	2	0	0	0
20.75	116.75	2	0	0	0
21	117	2	0	0	0
21.25	117.25	2	0	0	0
21.5	117.5	2	0	0	0
21.75	117.75	2	0	0	0
22	118	1	1	0	0
22.25	118.25	1	0	1	0
22.5	118.5	1	0	1	0
22.75	118.75	1	0	1	0
23	119	1	0	1	0
23.25	119.25	1	0	1	0
23.5	119.5	1	0	1	0
23.75	119.75	1	0	1	0
0	120	1	0	1	0
0.25	120.25	1	0	1	0
0.5	120.5	0	0	1	0
0.75	120.75	0	0	1	0
1	121	0	0	1	0
1.25	121.25	0	0	1	0
1.5	121.5	0	0	1	0
1.75	121.75	0	0	1	0
2	122	0	0	1	1
2.25	122.25	0	0	2	0
2.5	122.5	0	0	2	0
2.75	122.75	0	0	2	0
3	123	0	0	2	0
3.25	123.25	0	0	2	0
3.5	123.5	0	0	2	0
3.75	123.75	0	0	2	0
4	124	0	0	2	0
4.25	124.25	0	0	2	0
4.5	124.5	0	0	2	0
4.75	124.75	0	0	2	0
5	125	0	0	2	0
5.25	125.25	0	0	2	0
5.5	125.5	0	0	2	0
5.75	125.75	0	0	2	0

6	126	0	0	2	0
6.25	126.25	0	0	2	0
6.5	126.5	0	0	2	0
6.75	126.75	0	0	2	0
7	127	0	0	2	0
7.25	127.25	0	0	2	0
7.5	127.5	0	0	2	0
7.75	127.75	0	0	2	0
8	128	0	0	1	1
8.25	128.25	0	1	1	0
8.5	128.5	0	1	1	0
8.75	128.75	0	1	1	0
9	129	0	0	2	0
9.25	129.25	0	0	2	0
9.5	129.5	0	0	2	0
9.75	129.75	0	0	2	0
10	130	0	0	1	1
10.25	130.25	1	0	1	0
10.5	130.5	1	0	1	0
10.75	130.75	1	0	1	0
11	131	1	0	1	0
11.25	131.25	0	1	1	0
11.5	131.5	0	1	1	0
11.75	131.75	1	0	1	0
12	132	0	0	1	0
12.25	132.25	0	0	1	0
12.5	132.5	1	0	1	0
12.75	132.75	1	0	1	0
13	133	0	1	0	0
13.25	133.25	0	1	0	0
13.5	133.5	1	0	0	1
13.75	133.75	1	0	0	1
14	134	1	0	0	1
14.25	134.25	2	0	0	0
14.5	134.5	2	0	0	0
14.75	134.75	2	0	0	0
15	135	2	0	0	0
15.25	135.25	2	0	0	0
15.5	135.5	2	0	0	0
15.75	135.75	2	0	0	0
16	136	2	0	0	0
16.25	136.25	2	0	0	0
16.5	136.5	2	0	0	0
16.75	136.75	2	0	0	0
17	137	1	0	1	0
17.25	137.25	1	0	1	0
17.5	137.5	1	0	1	0
17.75	137.75	1	0	1	0
18	138	4	0	0	1
18.25	138.25	4	1	0	0
18.5	138.5	4	1	0	0

18.75	138.75	4	1	0	0
19	139	1	0	0	0
19.25	139.25	1	1	0	0
19.5	139.5	1	1	0	0
19.75	139.75	1	1	0	0
20	140	5	0	0	0
20.25	140.25	5	0	0	0
20.5	140.5	5	0	0	0
20.75	140.75	5	0	0	0
21	141	1	0	0	1
21.25	141.25	1	0	1	0
21.5	141.5	1	0	1	0
21.75	141.75	1	0	1	0
22	142	1	0	1	0
22.25	142.25	1	0	1	0
22.5	142.5	1	0	1	0
22.75	142.75	1	0	1	0
23	143	1	0	1	0
23.25	143.25	1	0	1	0
23.5	143.5	1	0	1	0
23.75	143.75	1	0	1	0
0	144	1	0	1	0
0.25	144.25	1	0	1	0
0.5	144.5	1	0	1	0
0.75	144.75	0	0	1	0
1	145	0	0	1	0
1.25	145.25	0	0	1	0
1.5	145.5	0	0	1	0
1.75	145.75	0	0	1	0
2	146	0	0	1	0
2.25	146.25	0	0	1	0
2.5	146.5	0	0	1	0
2.75	146.75	0	0	1	0
3	147	0	0	1	1
3.25	147.25	0	0	2	0
3.5	147.5	0	0	2	0
3.75	147.75	0	0	2	0
4	148	0	0	2	0
4.25	148.25	0	0	2	0
4.5	148.5	0	0	2	0
4.75	148.75	0	0	2	0
5	149	0	0	2	0
5.25	149.25	0	0	2	0
5.5	149.5	0	0	2	0
5.75	149.75	0	0	2	0
6	150	0	0	2	0
6.25	150.25	0	0	2	0
6.5	150.5	0	0	2	0
6.75	150.75	0	0	2	0
7	151	0	0	2	0
7.25	151.25	0	0	2	0

7.5	151.5	0	0	2	0
7.75	151.75	0	0	2	0
8	152	0	0	2	0
8.25	152.25	0	0	2	0
8.5	152.5	0	0	2	0
8.75	152.75	0	0	2	0
9	153	0	0	2	0
9.25	153.25	0	0	2	0
9.5	153.5	0	0	2	0
9.75	153.75	0	0	2	0
10	154	0	0	0	2
10.25	154.25	1	1	0	0
10.5	154.5	1	1	0	0
10.75	154.75	1	0	0	1
11	155	1	0	1	0
11.25	155.25	1	0	1	0
11.5	155.5	1	0	1	0
11.75	155.75	1	0	1	0
12	156	1	0	1	0
12.25	156.25	1	0	1	0
12.5	156.5	0	0	1	0
12.75	156.75	0	0	1	0
13	157	1	1	0	0
13.25	157.25	1	1	0	0
13.5	157.5	0	0	1	1
13.75	157.75	0	0	2	0
14	158	0	1	1	0
14.25	158.25	0	1	1	0
14.5	158.5	0	1	1	0
14.75	158.75	1	0	1	0
15	159	1	0	1	0
15.25	159.25	1	0	1	0
15.5	159.5	1	0	1	0
15.75	159.75	1	0	1	0
16	160	1	0	1	0
16.25	160.25	1	0	1	0
16.5	160.5	1	0	1	0
16.75	160.75	1	0	1	0
17	161	1	0	1	0
17.25	161.25	1	0	1	0
17.5	161.5	1	0	1	0
17.75	161.75	1	0	1	0
18	162	1	1	0	0
18.25	162.25	1	1	0	0
18.5	162.5	0	1	0	1
18.75	162.75	0	1	0	1
19	163	0	1	1	0
19.25	163.25	0	1	1	0
19.5	163.5	0	1	1	0
19.75	163.75	0	1	1	0
20	164	0	1	1	0

20.25	164.25	0	1	1	0
20.5	164.5	0	1	1	0
20.75	164.75	1	0	1	0
21	165	1	0	1	0
21.25	165.25	1	0	1	0
21.5	165.5	1	0	1	0
21.75	165.75	1	0	1	0
22	166	1	0	1	0
22.25	166.25	1	0	1	0
22.5	166.5	1	0	1	0
22.75	166.75	1	0	1	0
23	167	1	0	1	0
23.25	167.25	1	0	1	0
23.5	167.5	1	0	1	0
23.75	167.75	1	0	1	0

Bibliography

[1] Intergovernmental Panel on Climate Change. (2018) Special Report on Global Warming of 1.5 C (SR15). http://www.ipcc.ch/report/sr15/

[2] The European Parliament and the Council of the European Union. (2018) DIRECTIVE (EU) 2018/844 OF THE EUROPEAN PARLIAMENT AND OF THE COUNCIL of 30 May 2018 amending Directive 2010/31/EU on the energy performance of buildings and Directive 2012/27/EU on energy efficiency. Official Journal of the European Union, L 156/75. https://eur-lex.europa.eu/legal-content/EN/TXT/PDF/?uri=CELEX:32018L0844&from=EN

[3] Van den Dobbelsteen, A., Tillie, N. (2009) Towards CO2 Neutral Urban Planning: Presenting the Rotterdam Energy Approach and Planning (REAP). Journal of Green Building 4. http://www.isocarp.net/Data/case_studies/1488.pdf

[4] Menkveld, M., Matton, R., Segers, R., Vroom, J., Kremer, A.M. (2017) Monitoring warmte 2015. Centraal Bureau voor de Statistiek. https://www.cbs.nl/-/media/_pdf/2017/15/monitoringwarmte2015.pdf

[5] Badgwell, T.A., Qin, S.J. (2003) A survey of industrial model predictive control technology. Control Engineering Practice. vol. 11, pp. 733-764. https://doi.org/10.1016/S0967-0661(02)00186-7

[6] Alders, N., (2016) Adaptive thermal comfort opportunities for dwellings: Providing thermal comfort only when and where needed in dwellings in the Netherlands.

[7] Mohammad, H.H., Alsaleem, F., Rafaie, M., (2016) Sensitivity study for the PMV thermal comfort model and the use of wearable devices biometric data for metabolic rate estimation. Building and Environment.

[8] Seidner, A., (1999) Sick Building Syndrome. Hospital Practice.

[9] Lindelöf, D., Afshari, H., Alisafaee, M. Biswas, J., Caban, M., Mocellin, X., Viaene, J. (2015) Field tests of an adaptive, model-predictive heating controller for residential buildings. Energy and Buildings.

[10] Fanger, P.O. (1970) Thermal Comfort: Analysis and Applications In Environmental Engineering.

[11] Alders, N., Kurvers, S., Van den Ham, E. (2011) Adaptive Principles for Thermal Comfort in Dwellings - From Comfort Temperatures to Avoiding Discomfort. Proceedings of PLEA 2011, Architecture and Sustainable Development, p.p. 601-606.

[12] Nicol, J.F., Humphreys, M.A. (2002) Adaptive thermal comfort and sustainable thermal standards for buildings. Energy and buildings. https://doi.org/10.1016/S0378-7788(02)00006-3

[13] Ioannou, A., Itard, L., Agarwal, T. (2018) In-situ real time measurements of thermal comfort and comparison with the adaptive comfort theory in Dutch residential dwellings. Energy and Buildings. vol. 170, pp. 229-241. https://doi.org/10.1016/j.enbuild.2018.04.006

[14] Ioannou, A., Itard, L. (2017) In-situ and real time measurements of thermal comfort and its determinants in thirty residential dwellings in the Netherlands. Energy and Buildings. vol. 139, pp. 487-505. https://doi.org/10.1016/j.enbuild.2017.01.050

[15] Maasoumy, M., Razmara, M., Shahbakhti, M., Sangiovanni Vincentelli, A. (2014) Handling model uncertainty in model predictive control for energy efficient buildings. Energy and Buildings.

[16] Costanzo, G.T., Iacovella, S., Ruelens, F., Leurs, T., Claessens, B.J. (2016) Experimental analysis of data-driven control for a building heating system. Sustainable Energy Grids and Networks, vol. 6, pp. 81-90.

[17] Tanaskovic, M., Sturzenegger, D., Smith, R., Morari, M. (2017) Robust Adaptive Model Predictive Building Climate Control. IFAC-PapersOnLine, vol. 50, pp. 1871-1876. https://doi.org/10.1016/j.ifacol.2017.08.257

[18] Ferracuti, F., Fonti, A., Ciabattoni, L., Pizzuti, S., Arteconi, A., Helsen, L., Comodi, G. (2017) Data-driven models for short-term thermal behaviour prediction in real buildings. Applied Energy, vol. 204, pp. 1375-1387. https://doi.org/10.1016/j.apenergy.2017.05.015

[19] Baldi, S., Michailidis, I., Ravanis, C., Kosmatopoulos, E.B. (2015) Model-based and model-free plug-and-play building energy efficient control. Applied Energy, vol. 154, pp. 829-841. https://doi.org/10.1016/j.apenergy.2015.05.081

[20] Van Hoof, J., Mazej. M., Hensen, J.L.M. (2010) Thermal comfort: research and practice. Frontiers in Bioscience, vol. 15, pp. 765-788.

[21] Kim, J., Zhou, Y., Schiavon, S., Raftery, P., Brager, G. (2018) Personal comfort models: Predicting individuals' thermal preference using occupant heating and cooling behavior and machine learning. Building and Environment, vol. 129, pp. 96-106 https://doi.org/10.1016/j.buildenv.2017.12.011

[22] Van der Linden, A.C., Boerstra, A.C., Raue, A.K., Kurvers, S.R., De Dear, R.J. (2006) Adaptive temperature limits: A new guideline in The Netherlands: A new approach for the assessment of building performance with respect to thermal indoor climate. Energy and Buildings, vol. 38, pp. 8-17. https://doi.org/10.1016/j.enbuild.2005.02.008

[23] Peeters, L., De Dear, R., Hensen, J.L.M., D'haeseleer, W. (2009) Thermal comfort in residential buildings: Comfort values and scales for building energy simulation. Applied Energy, vol. 86, pp. 772-780 https://doi.org/10.1016/j.apenergy.2008.07.011

[24] Grubinger, T., Chasparis G.C., Natschläger, T. (2017) Generalized online transfer learning for climate control in residential buildings. Energy and Buildings, vol. 139, pp. 63-71. https://doi.org/10.1016/j.enbuild.2016.12.074

[25] Wetter, M., Bonvini, M., Nouidui, T.S. (2016) Equation-based languages A new paradigm for building energy modeling, simulation and optimization. Energy and Buildings, vol. 117, pp. 290-300. https://doi.org/10.1016/j.enbuild.2015.10.017

[26] Wetter, M., Van Treeck, C. (2016) New Generation Computational Tools for Building & Community Energy Systems - Annex 60 Final Report. International Energy Agency.

[27] U.S. Department of Energy. EnergyPlus. www.energyplus.net

[28] Abdullah, A., Cross, B., Aksamija, A. (2014) Whole Building Energy Analysis: A Comparative Study of Different Simulation Tools and Applications in Architectural Design. ACEEE Summer Study on Energy Efficiency in Buildings.

[29] U.S. Department of Energy. (2017) Getting Started. EnergyPlus Version 8.8.0 Documentation. https://energyplus.net/sites/all/modules/custom/nrel_custom/pdfs/pdfs_v8.8.0/GettingStarted.pdf. Retrieved at 31-01-2018.

[30] Trčka, M., Hensen, J.L.M. (2010) Overview of HVAC system simulation. Automation in Construction, vol. 19, pp. 93-99. https://doi.org/10.1016/j.autcon.2009.11.019

[31] MathWorks. Matlab/Simulink. https://nl.mathworks.com

[32] Functional Mock-up Interface. http://fmi-standard.org

[33] ITEA. (2010) Functional Mock-up Interface for Co-Simulation. https://svn.modelica.org/fmi/branches/public/specifications/v1.0/FMI_for_CoSimulation_v1.0.pdf

[34] Hafner, I., Rößler, M., Heinzl, B., Körner, A., Landsiedl, M. Breitenecker, F. (2014) Investigating communication and step-size behaviour for co-simulation of hybrid physical systems. Journal of Computational Science, vol. 5, pp. 427-438.

[35] Musić, J., Zupančič, B. (2015) Modeling, Simulation and Control of Inverted Pendulum on a Chart Using Object Oriented Approach with Modelica.

[36] Zuo, W., Wetter, M., Tian, W., Li, D., Jin, M., Chen, Q. (2016) Coupling indoor airflow, HVAC, control and building envelope heat transfer in the Modelica buildings library. Building Performance Simulation, vol. 9, pp. 366-381.

[37] Lawrence Berkeley National Laboratory, Modelica Buildings Library 5.0.1 (2017). http://simulationresearch.lbl.gov/modelica/index.html

[38] Rijksdienst voor Ondernemend Nederland (RVO), Referentiewoningen EPC = 0,4 (2015) https://www.rvo.nl/onderwerpen/duurzaam-ondernemen/gebouwen/wetten-en-regels-gebouwen/nieuwbouw/energieprestatie-epc/referentiewoningen-epc/tussenwoning

[39] Xu, Y. (2016) Modeling, Identification and Model Predictive Control Design for Multi-zone Thermal Control. University of Technology Eindhoven & AME.

[40] Tufa, D.L., Ramasamy, M. (2011) Closed-loop identification of systems with uncertain time delays using ARXOBF structure. Journal of Process Control. pp. 1148-1154.

[41] Wetter, M. Zuo, W., Nouidui, T.S. (2011) Modeling of Heat Transfer in Rooms in the Modelica "Buildings" Library. Proc. of the 12th IBPSA Conference, p. 1096-1103. Sydney, Australia, November 2011.

[42] Buildings documentation - Library with models for building energy and control systems http://simulationresearch.lbl.gov/modelica/releases/latest/help/Buildings.html.

[43] NEN1087 (2007). Ventilatie van gebouwen - Bepalingsmethoden voor nieuwbouw. Delft, ICS. 1087.

[44] Rawlings, J.B., Angeli, D., Bates, C.N. (2012) Fundamentals of Economic Model Predictive Control. Proceedings of the IEEE Conference on Decision and Control. pp. 3851-3861. https://ieeexplore-ieee-org.dianus.libr.tue.nl/stamp/stamp.jsp?tp=&arnumber=6425822

[45] Liu S., Liu J. (2016) Economic model predictive control with extended horizon. Automatica. Vol. 73, pp. 180-192. https://doi.org/10.1016/j.automatica.2016.06.027

[46] Löfberg, J. (2004) YALMIP : A Toolbox for Modeling and Optimization in MATLAB. In Proceedings of the CACSD Conference. https://yalmip.github.io/

[47] Dombrowski, J. (2015) McCormick envelopes. https://optimization.mccormick.northwestern.edu/index.php/McCormick_envelopes. *Retrieved at: 22-08-2018.*

[48] Gurobi Optimization, LLC. (2018) Gurobi Optimizer Reference Manual. http://www.gurobi.com.

[49] Jaga (2016) Jaga Catalogus Nederland. http://www.jagapro.nl/sites/default/files/tools/pdf/Jaga_Prijslijst_NL.pdf

[50] Akaike, H. (1974) A New Look at the Statistical Model Identification. IEEE Transactions on Automatic Control, vol. 19, pp. 716-722. https://ieeexplore-ieee-org.dianus.libr.tue.nl/stamp/stamp.jsp?tp=&arnumber=1100705.